Article:
Nicholls, H.C.G., Mallinson, H.E.H. orcid.org/0000-0001-9676-2285, Rolfe, S.A. orcid.org/0000-0003-2141-4707 et al. (3 more authors) (2020) Influence of contaminant exposure on the development of aerobic ETBE biodegradation potential in microbial communities from a gasoline-impacted aquifer. Journal of Hazardous Materials, 388. 122022. ISSN 0304-3894

https://doi.org/10.1016/j.jhazmat.2020.122022

Journal of Hazardous Materials 388 (2020) 122022

Contents lists available at ScienceDirect

Journal of Hazardous Materials

journal homepage: www.elsevier.com/locate/jhazmat

Influence of contaminant exposure on the development of aerobic ETBE biodegradation potential in microbial communities from a gasoline-impacted aquifer

H.C.G. Nicholls[a], H.E.H. Mallinson[a], S.A. Rolfe[b], M. Hjort[c], M.J. Spence[c,1], S.F. Thornton[a,*]

[a] Groundwater Protection and Restoration Group, Dept of Civil and Structural Engineering, University of Sheffield, Sheffield S1 3JD, United Kingdom
[b] Dept of Animal and Plant Sciences, Alfred Denny Building, University of Sheffield, Sheffield S10 2TN, United Kingdom
[c] Concawe, Environmental Science for European Refining, Boulevard du Souverain 165, 1160 Brussels, Belgium

GRAPHICAL ABSTRACT

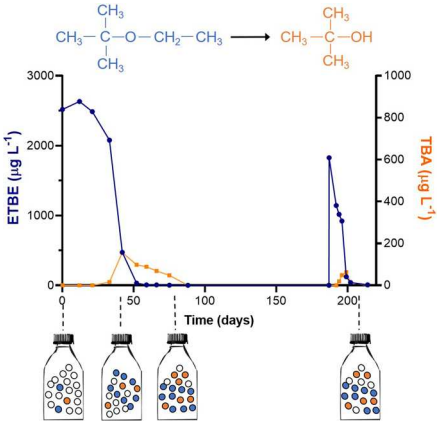

ARTICLE INFO

Editor: R. Debora

Keywords:
Gasoline ether oxygenates (GEO)
Bioremediation
Aquifer
ethB
Natural attenuation

ABSTRACT

Aerobic biodegradation of ethyl *tert* butyl ether (ETBE) in a gasoline-impacted aquifer was investigated in laboratory microcosms containing groundwater and aquifer material from ETBE-impacted and non-impacted locations amended with either ETBE, or ETBE plus methyl *tert* butyl ether (MTBE). As sole substrate, ETBE was biodegraded (maximum rate of 0.54 day^{-1}) without a lag in ETBE-impacted microcosms but with a lag of up to 66 days in non-impacted microcosms (maximum rate of 0.38 day^{-1}). As co-substrate, ETBE was biodegraded preferentially (maximum rate of 0.25 and 0.99 day^{-1} in non-impacted and impacted microcosms, respectively) before MTBE (maximum rate of 0.24 and 0.36 day^{-1} in non-impacted and impacted microcosms, respectively). Further addition of ETBE and MTBE reduced lags and increased biodegradation rates. *ethB* gene copy numbers increased significantly (> 100 fold) after exposure to ETBE, while overall cell numbers remained constant, suggesting that *ethB*-containing microorganisms come to dominate the microbial communities. Deep sequencing of 16S rRNA genes identified members of the Comamonadaceae family that increased in relative abundance upon exposure to ETBE. This study demonstrates the potential for ETBE biodegradation within the unsaturated

* Corresponding author
E-mail address: s.f.thornton@sheffield.ac.uk (S.F. Thornton).
[1] Present address: British Geological Survey, Environmental Science Centre, Keyworth, Nottingham, NG12 5GG, United Kingdom

https://doi.org/10.1016/j.jhazmat.2020.122022
Received 9 October 2019; Received in revised form 14 December 2019; Accepted 2 January 2020
Available online 03 January 2020

and saturated zone, and that ETBE biodegrading capability is rapidly developed and maintained within the aquifer microbial community over extended timescales.

1. Introduction

Gasoline ether oxygenates (GEO) are petroleum additives used to enhance fuel combustion and reduce emissions. Methyl *tert*-butyl ether (MTBE) is the most commonly used GEO worldwide. However, it has now been replaced in many European markets by ethyl *tert*-butyl ether (ETBE) at up to 15 vol% in formulations (Schuster et al., 2012), in response to the requirements of the EU Renewable Energy Directives (2009/28/EC), and synthesis of ETBE from (bio)ethanol for use in biofuels. ETBE may be released into the subsurface through accidental release at refineries, during transportation, storage or dispensing at filling stations, either as a pure chemical or, more commonly, as a component of gasoline together with benzene, toluene, ethylbenzene and xylene (BTEX) and other hydrocarbons (Shih et al., 2004; Stupp et al., 2012; van der Waals et al., 2018). An individual gasoline release will generally contain BTEX and a single GEO, but if repeated releases have occurred at a site, fuel blending practices may result in the contaminant plume containing multiple GEO. In the latter case a zone of mixed GEO-impacted groundwater may develop, in which the GEO plumes can be more persistent and extend further than the plumes of other gasoline components (Deeb et al., 2001; Fayolle-Guichard et al., 2012; Kulkarni et al., 2018). The main driver for GEO remediation is the low odour and taste thresholds in water. In Europe, advisory thresholds of 7–16 μg L^{-1} MTBE and 1–2 μg L^{-1} ETBE have been proposed (van Wezel et al., 2009), whereas the USEPA uses a threshold value of 20–40 μg L^{-1} for MTBE for all GEO in the U.S. (Environmental Protection Agency, 1997). Above these thresholds water is unpalatable, whereas the toxicity properties are less of a concern, with toxicity thresholds considerably higher than thresholds for taste and odour (Environmental Protection Agency, 1997).

The biodegradation of MTBE in groundwater has been well characterised (Deeb et al., 2000; Fayolle et al., 2001; Fiorenza and Rifai, 2003; Davis and Erickson, 2004; Stupp et al., 2012; Hyman, 2013). However, the aerobic biodegradation potential of ETBE and mixtures of ETBE with MTBE in groundwater remains poorly understood. While aerobic biodegradation of ETBE by cultured organisms has been reported in laboratory studies (Hernandez-Perez et al., 2001; Malandain et al., 2010; Le Digabel et al., 2013, 2014), this has rarely been described using gasoline-contaminated site material (van der Waals et al., 2019). In mixtures with other GEO, ETBE is reported to be biodegraded preferentially, before MTBE and tertiary amyl methyl ether (TAME) (Malandain et al., 2010). Molecular studies of *in situ* ETBE-degrading communities in gasoline-impacted groundwater are limited but important to identify specific microorganisms and associated genes for subsequent screening of ETBE biodegradation potential in aquifers. This knowledge may support the implementation of risk-based remediation concepts for ETBE-impacted aquifers, such as natural attenuation, and the design of bioremediation schemes for treatment of ETBE-impacted groundwater. However, the microorganisms responsible for aerobic biodegradation of ETBE in aquifers are not currently well characterised and the variability in aquifer microbial community degradation potential for ETBE has not been comprehensively documented. Microorganisms known to fully biodegrade MTBE include *Methylibium petroleiphilum* PM1 (Hanson et al., 1999) and *Methylibium* sp. R8 (Rosell et al., 2007), containing the MTBE monooxygenase, encoded by the *mdpA* gene, but this has no known activity towards ETBE. The first identified aerobic ETBE-degrader was *Rhodococcus ruber* IFP 2001 (Fayolle et al., 1998; Chauvaux et al., 2001). This microorganism can partially biodegrade ETBE to *tert*-butyl alcohol (TBA) under aerobic conditions (Rohwerder et al., 2006). Other microorganisms that can mineralise ETBE and TBA to biomass and CO_2 include *Betaproteobacteria* IFP 2047 (Le Digabel et al., 2014) and *Aquincola tertiaricarbonis* L108 (Rohwerder et al., 2006). Where ETBE is only partially biodegraded to TBA, commensal interactions within communities are important for complete substrate removal. For example, *Bradyrhizobium* sp. IFP 2049 can degrade TBA in a mixed consortia with *Rhodococcus* sp. IFP 2042, which first degrades ETBE to TBA (Le Digabel et al., 2013). The *ethRABCD* gene cluster, which is responsible for initiating ETBE biodegradation, includes a positive transcriptional regulator (*ethR*) and a cytochrome P450 monooxygenase (*ethB*) (Chauvaux et al., 2001). The cytochrome encoded by the *ethB* gene is responsible for oxygen incorporation during initial GEO biodegradation. Unlike MTBE, ETBE interacts with the regulator (*ethR*), inducing *ethB* expression, whereas the *eth*B-encoded cytochrome has activity towards ETBE, MTBE and TAME, with ETBE degraded preferentially in a mixture with other GEO (Malandain et al., 2010). The detection of the *ethB* gene is important to confirm ETBE biodegradation capability at an ETBE release site and there is also a requirement for dissolved oxygen, given that this gene encodes a monooxygenase. ETBE biodegradation in groundwater therefore occurs outside the anaerobic BTEX-contaminated zone. While aerobic biodegradation of ETBE has been reported in several studies, there is limited evidence for anaerobic biodegradation of ETBE in soils using NO_3- as an electron acceptor (Yeh and Novak, 1994), under mixed redox conditions (Bombach et al., 2015) and with other organic co-contaminants (van der Waals et al., 2018).

The biodegradation of many gasoline constituents in groundwater, including hydrocarbons and GEO, is influenced by contaminant exposure history (Feris et al., 2004; Shah et al., 2009; Le Digabel et al., 2014), heterogeneity in the distribution of contaminants and microorganisms (Medihala et al., 2012) and *in situ* conditions, such as oxygen availability (Franklin et al., 1999). A zone of contaminated material commonly develops across the unsaturated-saturated zone interface in gasoline-impacted aquifers due to vertical displacement of gasoline caused by water table fluctuations. This zone is likely to be characterised by a spatial variation in the distribution of both organic compounds and dissolved oxygen with depth (Stafford and Rixey, 2012; Xu et al., 2015), which can be hypothesised to influence the distribution and community structure of microorganisms responsible for aerobic biodegradation between the unsaturated zone and saturated zone. Similarly, it is well known that microbial activity and biodegradation potential vary spatially across the interface (plume fringe) between a contaminant plume and non-impacted groundwater in response to gradients between substrates, dissolved oxygen and redox processes created by dispersion and diffusion (Thornton et al., 2001; Pickup et al., 2001; Tuxen et al., 2006). Numerous studies have also highlighted different microbial community structures in relation to depth in soil (Blume et al., 2002; Eilers et al., 2012) and aquifers (Lima et al., 2018), but the spatial variation in ETBE biodegradation potential in aquifers is unknown.

The aim of this study was to examine the influence of contaminant exposure history and spatial-temporal variation in microbial community composition on the development of aerobic ETBE biodegradation potential, by an aquifer microbial community exposed to ETBE at a gasoline-release site. The influence of prior exposure to ETBE was compared for locations in the aquifer which were impacted and not impacted by the gasoline release at the time of sampling, and for situations in which ETBE was present as the only substrate or as a co-substrate with MTBE. These experiments sought to simulate different release scenarios (ETBE-only vs mixed GEO-impacted groundwater) that could occur. The effect of spatial variability in microbial

community composition was examined by comparing different depths in impacted/non-impacted locations and across the unsaturated zone-saturated zone interface of the ETBE-impacted aquifer. In each case, the aerobic biodegradation of ETBE was characterised with respect to biodegradation lag and rates, the abundance of GEO biodegrading genes and changes in the microbial community composition after repeated exposure to ETBE and/or ETBE/MTBE, and subsequent persistence of aerobic ETBE-biodegrading microorganisms.

2. Methods

2.1. Site geology, hydrogeology and sample collection

Groundwater and aquifer material samples were collected from an ETBE-impacted site in France to construct laboratory microcosms. The aquifer comprises Quaternary alluvial deposits, with up to 3 m gravel sandy loam underlain by 3–5 m clay loam and 5–20 m gravel and sand. Groundwater flow is towards the south west (Fig. 1), with a water table that fluctuates between 7 and 10 m below ground level (BGL).

Two locations were selected to provide inocula for the laboratory experiments; a non-impacted location (N), upgradient of the ETBE-impacted zone, where ETBE and BTEX compounds were below detection limits, and an impacted location (I) in the ETBE-impacted zone, according to groundwater chemistry from the corresponding piezometer monitoring well installed after coring (Fig. 1a). Cored samples of aquifer material were collected by sonic drilling (July 2016) and transferred to sterile (70% v/v ethanol-washed) 2.5 L gas-tight jars (Anaerocult, Merck), and stored at 4 °C. Aquifer material from the non-impacted location was sampled (Fig. 1b) at two depths (8–9 m, "x", and 13–14 m, "z") and from the impacted location at three depths (8–9 m, "x" 9–10 m, "y", and 13–14 m, "z"). Groundwater samples were collected (October 2016) from piezometer monitoring wells installed at these locations after coring, in autoclaved glass bottles filled completely and stored at standard temperature of 4 °C.

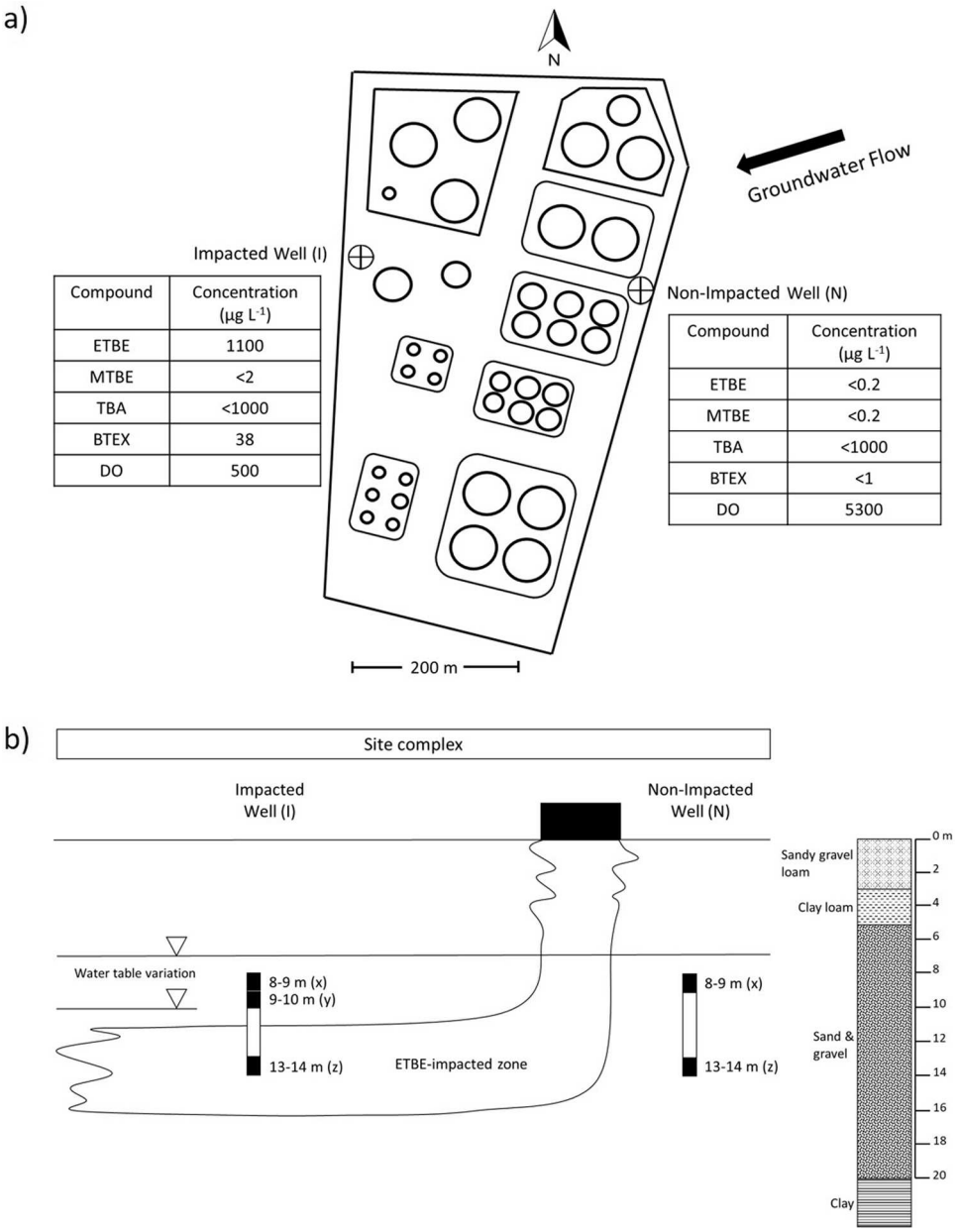

Fig. 1. a) Schematic site plan showing site infrastructure and location of core boreholes with installed monitoring wells (⊕) used for sampling. The tables show contaminant and dissolved oxygen (DO) concentration made at the time of sampling. b) conceptual cross section of site showing cored borehole/monitoring well locations and sampling depths (black bars). The black bars show depths from which aquifer material and groundwater were sampled.

Particle size analysis was completed on the aquifer material prior to constructing the laboratory microcosms. The material was first passed through a sterile 4 mm mesh to remove large solids and thoroughly mixed before been placed into a microcosm. The remaining aquifer material was dried at 105 °C for 48 h and the particle size distribution determined using a mechanical shaker for 20 min with steel sieves (< 63, 63–150, 150–212, 212–300, 300–425, 425–600, 600–1180 and 1180–2400 µm).

2.2. Laboratory microcosms

Groundwater and aquifer material used to construct the laboratory microcosms were handled and processed under sterile conditions. A 130 g sample of 4 mm sieved aquifer material and 650 mL of groundwater were placed into autoclaved 1 L Duran bottles to create replicate live and sterile controls in each experiment (Table 1). Sterile controls were created by the addition of 2 g L^{-1} (w/v) sodium azide to the groundwater. The microcosms were sealed with chemically inert gas-tight caps with 3 sampling ports (PTFE, Q-Series, Diba) to minimise abiotic losses and the headspace of each bottle flushed with filter-sterilised (0.2 µm PES, Millex) N_2 (BOC gases). A mass balance calculation, based on gas partitioning according to Henrys Law for aqueous and gas phase distributions, was used to adjust the dissolved oxygen (DO) concentration in each microcosm to a nominal value of 2 mg L^{-1} with either filter-sterilised (0.2 µm PES, Millex) O_2 or N_2 (BOC gases). The DO concentration was measured using a remote sensing system (Presens GmbH, Germany) as described previously (Shah et al., 2009). After DO addition the microcosms were equilibrated for 48 h before ETBE (99% purity, Sigma) or MTBE (99% purity, Sigma) was added at a nominal concentration of between 2000–3000 µg L^{-1}. The microcosms were incubated in the dark at 12 °C (the groundwater temperature at the field site).

Groundwater samples were taken at intervals for the analysis of organic compounds and inorganic ions. All microcosms were mixed gently to remove solute concentration gradients and allowed to warm to room temperature for two hours before sampling. After measurement of DO, 1 mL of groundwater was extracted via the sampling port using a sterile syringe and discarded to flush the sample line before a sample for analysis was collected. Groundwater samples for ETBE, MTBE and TBA analysis were analysed immediately using GC–MS (section 2.3). Groundwater samples for the analysis of major ions and metals (dissolved iron and manganese) were filtered (0.2 µm PES, Millex) and stored at 4 °C until analysis. Samples for metal analysis were preserved by acidification (1% (v/v) HCl) after filtration. Samples for molecular analysis were obtained by gently swirling the microcosms to suspend the aquifer material and immediately collecting a slurry (mixed groundwater-aquifer material) sample. After sample removal, an equal volume of filter-sterilised N_2 was added to each microcosm to prevent a negative headspace pressure.

2.3. Chemical analysis

The analysis of MTBE, ETBE and TBA was performed by solid phase micro-extraction (SPME) of the aqueous phase using a CombiPAL autosampler (CTC Analytics AG, Zwingen, Switzerland) connected to a Shimadzu QP1000 GC–MS. SPME was carried out using an 85 µm Carboxen/PDMS StableFlex SPME fibre (Supelco, UK), with an extraction time of 2 min in the aqueous sample. The fibre was desorbed in the injection port of the GC–MS at 300 °C for 3 min. The GC–MS was fitted with a DB-624 capillary column (121–1324, Agilent Technologies Ltd), with an initial oven temperature of 40 °C. The temperature was increased at 10 °C min^{-1} to 170 °C, then at 40 °C min^{-1} to 250 °C, then held for 2 min, for a total run time of 17 min. The column flow was 1.18 mL min^{-1}, using Helium as the carrier gas, with a split ratio of 30:1. The GC–MS interface was set to 250 °C, with the GC–MS ion source at 200 °C and solvent cut time of 1.4 min. The MS programme was set to Scan/SIM mode, allowing for a full scan of the *m/z* values 30–200 alongside monitoring of selected ions corresponding to the retention times of each analyte. In addition to calibration standards, an internal standard containing deuterated isotopologues of the analytes of interest was also prepared (Supplementary Table S1). The peak area represented by the quantification ion was used to calculate the concentration of the analyte in the original sample. The ratio of the peak areas of the quantification and reference ions and the retention time was used to identify the analyte peak, using GC-MSsolution V2 software (Shimadzu). A typical chromatogram showing the target compounds and internal standards is provided in Supplementary Figure S1).

Dissolved major ions were analysed using a Dionex 3000 instrument equipped with cation and anion modules for simultaneous detection. Anions (SO_4^{2-}, NO_3^-, $NO_2^-$and PO_4^{3-}) were analysed on an AS18 column with an AG18 guard column, whereas cations (Ca^{2+}, Mg^{2+}, K^+ and Na^+) were analysed on a CS12A column with a CG12A guard column. The anion eluent was 34 mM potassium hydroxide with a flow rate of 0.2 mL min^{-1} and the cation eluent was 28 mM methane sulphonic acid with a flow rate of 0.4 mL min^{-1}. A 10 µL sample was injected. The instrument was calibrated before each analysis using high purity reagent and standard metal solutions (Fisher Scientific), with independent analytical quality controls analysed after every 10 samples.

Samples for the analysis of total Fe and Mn were diluted 1:10 in 1% (v/v) HNO_3. The calibration standards, samples and quality control standards were run on a Perkin Elmer Elan DRCII instrument with ICP power at 1300 W. Argon flow through the nebulizer was 0.85 L min^{-1}, coolant flow was 15 L min^{-1}, plasma flow was 0.5 L min^{-1} and the solution was pumped at 2.5 mL min^{-1}. Detection was by a solid-state diode array device and all element emission wavelengths were measured simultaneously. Quality control standards were run after every 10 samples.

2.4. Microscopy

Images of aquifer material grains were acquired from microcosm slurry samples. The grains were gently washed twice with 10 mM NaCl. After removal of supernatant 200 µL of 6 µM SYTO 9 Green fluorescent stain (Thermo) was mixed with the grains and incubated in the dark for 15 min. Z-stack images were obtained using a Leica DM6 fluorescence

Table 1
Matrix showing experiment identification labels for live and sterile bottles, the source of groundwater and aquifer material (including depth) and GEO additions made. Replicate numbers are shown in parentheses.

Experiment	Groundwater	Aquifer location and depth	GEO addition	Live microcosms	Sterile microcosms
N-X-E	N	'x' 8-9 m	ETBE	N-X-E (1-2)	N-X-E (3-4)
N-Z-E	N	'z' 13-14 m	ETBE	N-Z-E (1-3)	N-Z-E (4-5)
N-X-EM	N	'x' 8-9 m	ETBE and MTBE	N-X-EM (1-3)	N-X-EM (4-5)
I-X-E	I	'x' 8-9 m	ETBE	I-X-E (1-3)	I-X-E (4-6)
I-Y-E	I	'y' 9-10 m	ETBE	I-Y-E (1-3)	I-Y-E (4-6)
I-Z-E	I	'z' 13-14 m	ETBE	I-Z-E (1-3)	I-Z-E (4-6)
I-X-EM	I	'x' 8-9 m	ETBE and MTBE	I-X-EM (1-3)	I-X-EM (4-6)

microscope using excitation at 480 nm and emission at 500 nm.

Live/dead cell counts were performed using 100 µL of groundwater sample mixed with 10 mL of 10 mM NaCl and vacuum filtered through a black 0.2 µm filter membrane (Whatman). Bacteria were stained using Live/Dead Baclight bacteria viability kit (L7007, Thermo) according to the manufacturer's instructions. Counts were performed using a Leica DM6 fluorescence microscope and imaged using Leica Application Software X.

2.5. Molecular analysis

A 20 mL slurry sample (groundwater and suspended aquifer material) from each microcosm was filtered through a polycarbonate 0.1 µm membrane filter (Whatman) using a plastic syringe. Samples were stored at −80 °C prior to DNA extraction. DNA was extracted using FastDNA Spin kit for Soil (MP Biomedicals, UK) according to the manufacturer's instructions, with an additional 10 min incubation at 65 °C prior to homogenisation. DNA quantification was performed using Qubit dsDNA HS Assay (ThermoFisher, UK).

2.5.1. Quantitative real-time PCR (qRT-PCR)

2.5.1.1. Preparation of standards. The *eth* cluster (*ethABCD*) and *mdpA* genes were amplified from *Aquincola tertiaricarbonis* L108 and *Methylibium* sp. R8 respectively (organisms provided by Dr T Rohwerder, UFZ). Both organisms were cultured in Mineral Salts Medium (Rohwerder et al., 2006) at 20 °C with the addition of 0.5 g L^{-1} MTBE. Cells were pelleted and DNA extracted using the FastDNA kit for Soil. The *eth* gene cluster and *mdp*A genes were amplified by end-point PCR using MyTaq Mix (Bioline, UK) according to the manufacturer's instructions. PCRs were carried out using a Prime thermocycler (Techne, UK) under the following conditions: 95 °C for 5 min; 30 cycles of 95 °C for 30 s, annealing temperature according to primers used for 30 s, 72 °C for 1 min; and 72 °C for 5 min. A 3032 base pair (bp) section of the *ethABCD* gene cluster was amplified using primers eth_ABCD_F and eth_ABCD_R, and the *mdpA* gene was amplified using mdpA_1 F and mdpA_1R (Table 2). PCR products were electrophoresed through 1% (w/v) agarose gels, bands excised and purified using QIAquick PCR purification kit (Qiagen, UK), according to the manufacturer's instructions. The PCR products were quantified by UV spectrophotometry. Standards of the *eth* operon and *mdpA* gene were prepared at concentrations from 10^1 to 10^5 gene copies μL^{-1}. Each standard was mixed with 1 ng *E. coli* genomic DNA to provide a complex background. The standard for the 16S rRNA gene consisted of purified *E. coli* genomic DNA (0.0001–1 ng μL^{-1}).

2.5.1.2. qRT-PCR. Absolute quantification of *ethB*, *mdpA* and 16S rRNA gene copies was carried out using qRT-PCR. The primers used are shown in Table 2. qRT-PCR was performed on a Rotorgene (Corbett) using the SensiFast SYBR NO-ROX kit (Bioline, UK). qRT-PCR reactions were carried out according to manufacturer's instructions using 1 µL of DNA extract, in a reaction volume of 10 µL, under the following conditions; 95 °C for 3 min; 40 cycles of 95 °C for 10 s, annealing at specific primer temperature for 10 s (Table 2), 72 °C for 10 s. A melt curve was performed to check primer specificity. Primer specificity was also checked by gel electrophoresis using a 2% (w/v) agarose gel. Lower detection limits were determined; *ethB*, *mdpA* and 16S rRNA was 30, 14 and 19 gene copies per reaction respectively.

2.5.2. 16S rRNA gene sequencing

The 16S rRNA gene was amplified from the DNA extracts using MyTaq DNA polymerase (Bioline) with the universal prokaryotic primers Bakt341 and Bakt805 (Klindworth et al., 2013). PCRs were carried out using 2 µL of DNA extract, 0.4 µL of 10 µM primers and the manufacturer's buffer, with a final reaction volume of 20 µL, under the following conditions; 95 °C for 1 min; 26 cycles of 95 °C for 30 s, 55 °C for 30 s, 72 °C 30 s; and 72 °C for 1 min using a Prime thermocycler (Techne). Amplification was confirmed by gel electrophoresis using a 1.5% (w/v) agarose gel. Each sample was amplified in triplicate to minimise PCR bias and pooled.

PCR products were cleaned by mixing 24 µL of pooled sample with 20 µL Agencourt AMPure XP beads (Beckman) and incubated for 5 min at room temperature. Sample tubes were placed on to a magnetic rack and the supernatant removed once clear. Beads were washed twice with 80% (v/v) ethanol and resuspended in 10 mM Tris (pH 8.5). Index PCR was performed using a KAPA HiFi HS kit (Roche) and Nextera XT Index Kit Set A v2 (Illumina). PCRs used 5 µL of PCR product, 5 µL of each index primer, 1 µL $MgCl_2$ (25 mM), 1.5 µL dNTPs (10 mM each) and reaction buffer, with a final reaction volume of 50 µL, under the following conditions; 95 °C for 3 min; 8 cycles of 95 °C for 30 s, 55 °C for 30 s, 72 °C for 30 s; and 72 °C for 5 min. Amplifications were checked by gel electrophoresis using a 2% (w/v) agarose gel. Index PCR products were cleaned by mixing with 50.4 µL Agencourt AMPure XP beads, incubated for 5 min at room temperature and processed as described above. Index PCR products were quantified using QuantiFluor dsDNA system (Promega), diluted to 10 nM with 10 mM Tris and pooled.

16S rRNA amplicons were sequenced using an Illumina MiSeq producing 250 bp paired end reads. As the amplicon size was 465 bp, only 25–29 % of the sequences in each sample overlapped, so analysis was restricted to the forward primer sequences. Initial data processing was performed using usearch (Edgar, 2010) and Qiime (Caporaso et al., 2010b). Primer sequences were removed and the sequences filtered for quality with a maxEE value of 1. Chimeric sequences were identified using a combination of reference based and *de novo* algorithms and removed. A total of 7,121,912 sequences passed the quality filters and 7,109,219 were classed as non-chimeric. Operational Taxonomic Units (OTUs) were picked by clustering at 97% similarity using uclust (Edgar, 2010) and representative sequences compared using PyNAST (Caporaso et al., 2010a) with the Greengenes_13_8 database (DeSantis et al., 2006). Where taxonomies were incomplete, they were completed by taking the lowest taxonomic rank identified and adding 'sp' to the name. The resulting OTU count data and assigned taxonomies were assembled into a biom file and analysed further using R (R Core Team,

Table 2
End-point and qRT-PCR primers used, including sequence and annealing temperatures.

Gene	Primer ID	Sequence (5'-3')	Annealing temperature	Reference
ethABCD	eth_ABCD_F	CTGCGCGATCACGGCTATAC	57 °C	This study
	eth_ABCD_R	GCGACCATGTAGTACGGGAC		
mdpA	mdpA_1F	CTTACCGGGCTCAACTATGC	59 °C	Jechalke et al., 2011
	mdpA_1R	CGCTTCCCTGGATCGATGTT		
ethB	ethB_105_fwd	GGTGTCCAACACCGAGATG	62 °C	Malandain et al., 2010
	ethB_105_rev	CGGATGAGGTTGTTGATGTG		
mdpA	mdpA_192_fwd	GAGCGGAACTGGAGTCCTCA	63 °C	This study
	mdpA_192_rev	TCTGCATCTCCGTGGGTCTT		
16S rRNA	Bakt799_fwd	AACMGGATTAGATACCCKG	62 °C	Bodenhausen et al., 2013
	Bakt1193_rev	ACGTCATCCCCACCTTCC		

2018) and the phyloseq package (McMurdie and Holmes, 2013).

Taxa which could not be assigned to Bacteria or Archaea at the Kingdom level were removed leaving 32,281 distinct OTUs across the 92 samples. Samples reads varied between 39,066 and 141,482. This raw dataset was used for analysis of diversity. For analyses that required equal sequencing depth, a rarefied data set was produced, sampled to the lowest number of reads. Rarefaction curves (Supplementary Figure S2) showed sufficient sequencing depth to capture the majority of diversity in the samples.

For calculation of diversity indices, samples were rarefied to equal depth 10 times, indices calculated using the 'estimate_richness' function of phyloseq, and the average value calculated. Statistical differences between treatments were calculated using a generalised linear model of log normalised values. Differences between time points within a microcosm were calculated in the same way with a *post-hoc* Tukey test. Principal component analysis was performed using a weighted phylogenetically-aware Unifrac method (Lozupone et al., 2011) with the pairwise Adonis R package (Martinez Arbizu, 2019) used to determine which samples differed. Differentially abundant OTUs were identified using DESEQ2 (Love et al., 2014) using the parametric estimation of variance-mean dependence. The raw dataset was filtered before analysis, requiring a minimum of 30 total reads across all samples and presence at least 3 times in 20% of the samples. The filtered dataset contained 2112 unique OTUs. Significant results were reported after correction for false discovery with an adjusted p value of 0.05, and a mean score of 30 or more reads across all samples.

3. Results

3.1. GEO biodegradation

The biodegradation of each GEO was monitored over a 214 day period using microcosms established with groundwater and aquifer material sampled upgradient of the ETBE-impacted zone (referred to as non-impacted, N) or from the ETBE-impacted zone (referred to as impacted, I). The non-impacted material has no known history of ETBE exposure whilst the impacted location had 1100 μg L^{-1} ETBE and 38 μg L^{-1} BTEX in groundwater at the time of sampling (Fig. 1). The concentration of ETBE, MTBE, TBA and inorganic species (Supplementary Table S2) were determined in all microcosms prior to the initial GEO addition. Three additions of GEO were made to the impacted microcosms, whereas two additions were made to the non-impacted set, due to the different GEO biodegradation kinetics. GEO biodegradation was accompanied by the consumption of dissolved oxygen and the maximum slope of each GEO biodegradation profile, excluding the lag, was used to estimate the biodegradation rate with a first-order model (Table 3). The grain size distribution of aquifer material used in the microcosms is shown in Supplementary Figure S3. All samples were composed of well-sorted sand with a uniform grain size distribution and consistency between the sampling locations.

3.1.1. Biodegradation in microcosms amended with ETBE only

Biodegradation of ETBE in microcosms established with non-impacted groundwater and aquifer material (location N) from depth 'x' (8–9 m, which is above the water table) started after a mean lag of 66 days (Fig. 2a). The lag preceding biodegradation was reduced considerably after a second ETBE addition (12 days) and the first-order biodegradation rate increased for N-X-E1 (0.06 vs 0.32 day^{-1}) but was unchanged (0.22 day^{-1}) for N-X-E2 after the first and second ETBE addition (Table 3). No TBA accumulated in these microcosms.

Microcosms established using non-impacted groundwater and aquifer material from depth 'z' (13–14 m, which is below the water table) had a mean lag of 36 days prior to ETBE biodegradation (Fig. 2b). Biodegradation occurred with a first-order rate constant of 0.28 day^{-1} and there was a transient accumulation of TBA (16–157 μg L^{-1}). After 188 days ETBE was re-added to the microcosms. The lag preceding biodegradation was reduced (5 days) and TBA accumulated at a lower concentration (13–63 μg L^{-1}), but the biodegradation rate of 0.31 day^{-1} did not differ significantly from that of the first ETBE addition ($p = 0.52$). The nitrate, sulphate, iron and manganese concentrations remained constant (data not shown), implying that ETBE was biodegraded aerobically. No ETBE loss, TBA production or oxygen removal occurred in the sterile controls.

The lag prior to the onset of ETBE biodegradation in microcosms (depths 'x', 'y' and 'z') established with groundwater and aquifer material from the ETBE-impacted location (Well I) was less than 12 days, as biodegradation had commenced by the first sampling point and appeared nearly complete after 21 days (Fig. 3), with an average biodegradation rate of 0.29 day^{-1} (Table 3). ETBE was re-added to these microcosms after 42 days. This resulted in biodegradation with a lag of < 4 days and a mean biodegradation rate for all microcosms of 0.4 day^{-1}. ETBE was re-added to all microcosms after 188 days. Lag periods of 6–8 days were evident prior to ETBE biodegradation for microcosm sets 'x', 'y' and 'z'. However, the mean biodegradation rate was slower (0.23 day^{-1}) than that following the second ETBE addition ($p = 0.001$). TBA accumulated after the ETBE additions. In most cases the TBA concentration was less than 150 μg L^{-1}, except I-*Z*-E3 where TBA accumulated to 1227 μg L^{-1} after the first ETBE addition, coincident with very rapid ETBE biodegradation. In all microcosms, TBA accumulation was less following each subsequent ETBE addition.

Dissolved O_2 was above detection limits during the experiment for all microcosms but decreased rapidly following the second addition of ETBE. Concentrations of nitrate, sulphate, iron and manganese remained constant (data not shown), implying that ETBE was biodegraded aerobically. No ETBE loss, TBA production or oxygen removal occurred in the sterile controls.

3.1.2. Biodegradation in microcosms amended with ETBE and MTBE

Additional microcosms were established with ETBE and MTBE as co-substrates to examine the effect on ETBE biodegradation of a separate release of gasoline containing MTBE. These microcosms were established using the same source material as N-X-E and I-X-E, but with a nominal concentration of 1500–2000 μg L^{-1} of MTBE and ETBE added.

ETBE biodegradation in experiment N-X-EM started before MTBE. The lag preceding ETBE and MTBE biodegradation was between 45 and 60 days, with biodegradation rates of 0.19 and 0.13 day^{-1},

Table 3
First order biodegradation rates (day^{-1}) for all microcosm experiments, according to GEO amendment. Values indicated by "nd" could not be determined due to insufficient data.

	ETBE (day^{-1})			MTBE (day^{-1})		
Microcosm	1	2	3	1	2	3
N-X-E1	0.06	0.32	–			
N-X-E2	0.22	0.22	–			
N-Z-E1	0.24	0.26	–			
N-Z-E2	0.29	0.3	–			
N-Z-E3	0.32	0.38	–			
I-X-E1	0.34	0.4	0.36			
I-X-E2	0.35	0.53	0.18			
I-X-E3	0.33	0.54	0.36			
I-Y-E1	0.22	0.33	0.2			
I-Y-E2	0.22	0.39	0.27			
I-Y-E3	0.23	0.34	0.21			
I-Z-E1	0.3	0.34	0.23			
I-Z-E2	0.37	0.41	0.18			
I-Z-E3	nd	0.31	0.29			
N-X-EM1	0.25	0.19	–	0.16	0.24	–
N-X-EM2	0.21	0.25	–	0.13	0.16	–
N-X-EM3	0.11	0.14	–	0.1	nd	–
I-X-EM1	nd	0.95	0.25	nd	0.36	0.25
I-X-EM2	nd	0.59	0.39	nd	0.22	0.29
I-X-EM3	nd	0.99	0.32	nd	0.32	0.29

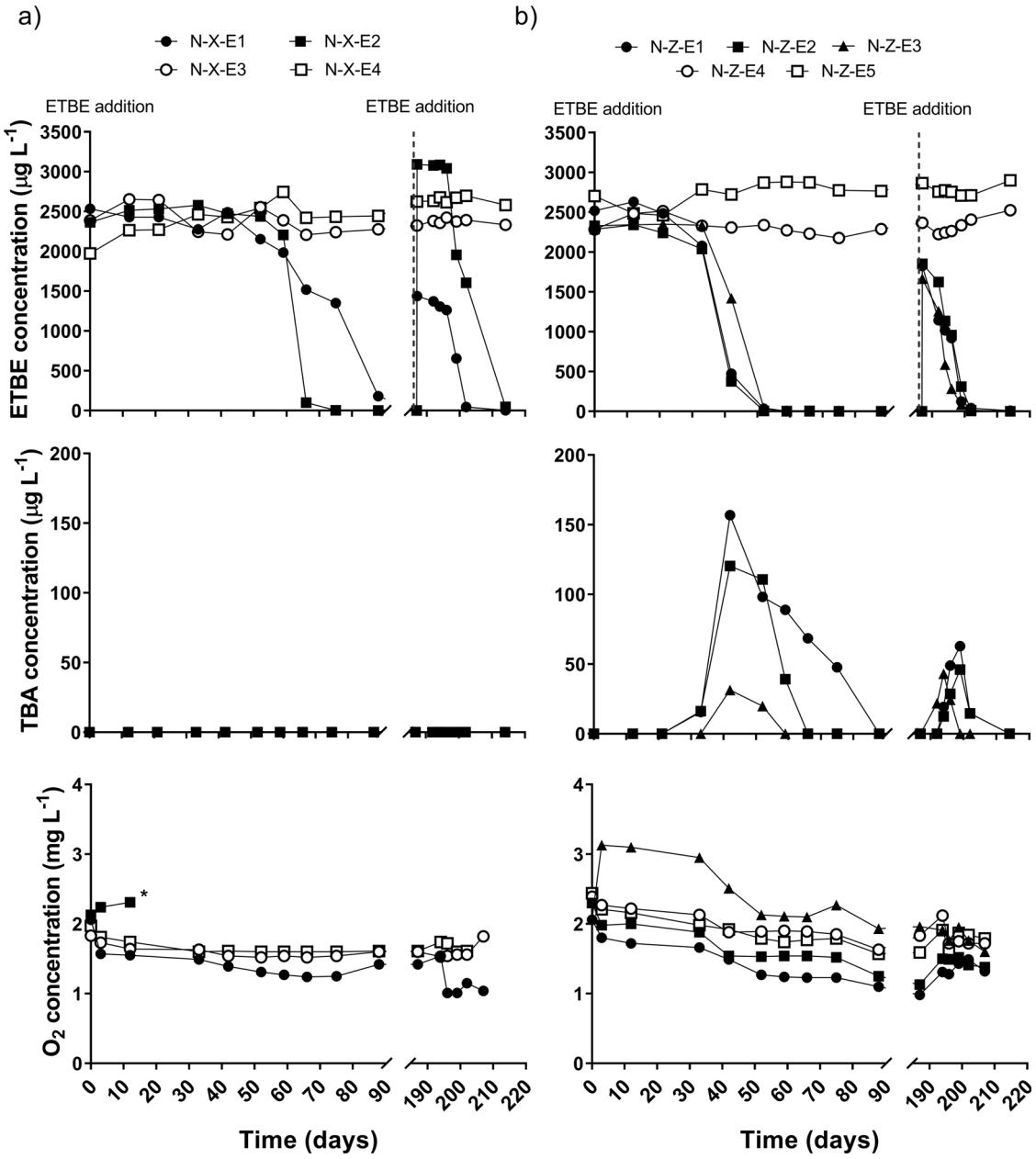

Fig. 2. ETBE, TBA and O_2 profiles for microcosms established using non-impacted (N) groundwater and aquifer material from a) depth 'x' (8–9 m) and b) 'z' (13–14 m) located upgradient of the ETBE-impacted zone. Solid symbols are live microcosms and open symbols are sterile controls. ETBE was added twice to the microcosms as indicated. * O_2 sensor failed beyond this point.

respectively. TBA (max 22 µg L^{-1}) was produced during biodegradation of ETBE and MTBE. There was a much shorter lag before ETBE and MTBE biodegradation after the second addition of GEO, although biodegradation rates were similar to the first GEO addition for both ETBE ($p = 0.95$) and MTBE ($p = 0.16$). TBA (~25 µg L^{-1}) was produced during biodegradation of the GEO (Fig. 4a).

In experiment I-X-EM1 ETBE was biodegraded without a lag (Fig. 4b), whereas MTBE biodegradation was delayed by 12 days. The second GEO amendment resulted in faster removal of each substrate (mean biodegradation rate of 0.84 day^{-1} for ETBE and 0.3 day^{-1} for MTBE) and ETBE biodegradation was completed before MTBE. The same behaviour was observed after the third addition of ETBE and MTBE, although the biodegradation rate for ETBE was reduced compared with the second addition ($p = 0.02$) and was not statistically significantly different for MTBE ($p = 0.62$). There was transient accumulation of TBA in all microcosms but to a lesser extent with each GEO addition. The third addition of GEO resulted in two distinct peaks of TBA production, corresponding with ETBE and MTBE biodegradation. The DO concentration decreased during biodegradation of the GEO, most rapidly during biodegradation of the second GEO addition, whereas the concentration of NO_3 and SO_4 remained unchanged (data not shown), confirming aerobic biodegradation of ETBE and MTBE. No GEO consumption, TBA production or oxygen removal occurred in the sterile controls.

Biodegradation of ETBE started before MTBE in both sets of microcosms, although the respective rates were comparable (Table 3). Furthermore, the maximum rate of MTBE biodegradation did not occur until most of the ETBE was removed, and MTBE was biodegraded only slowly when the ETBE concentration was relatively high (> 1000 µg L^{-1}).

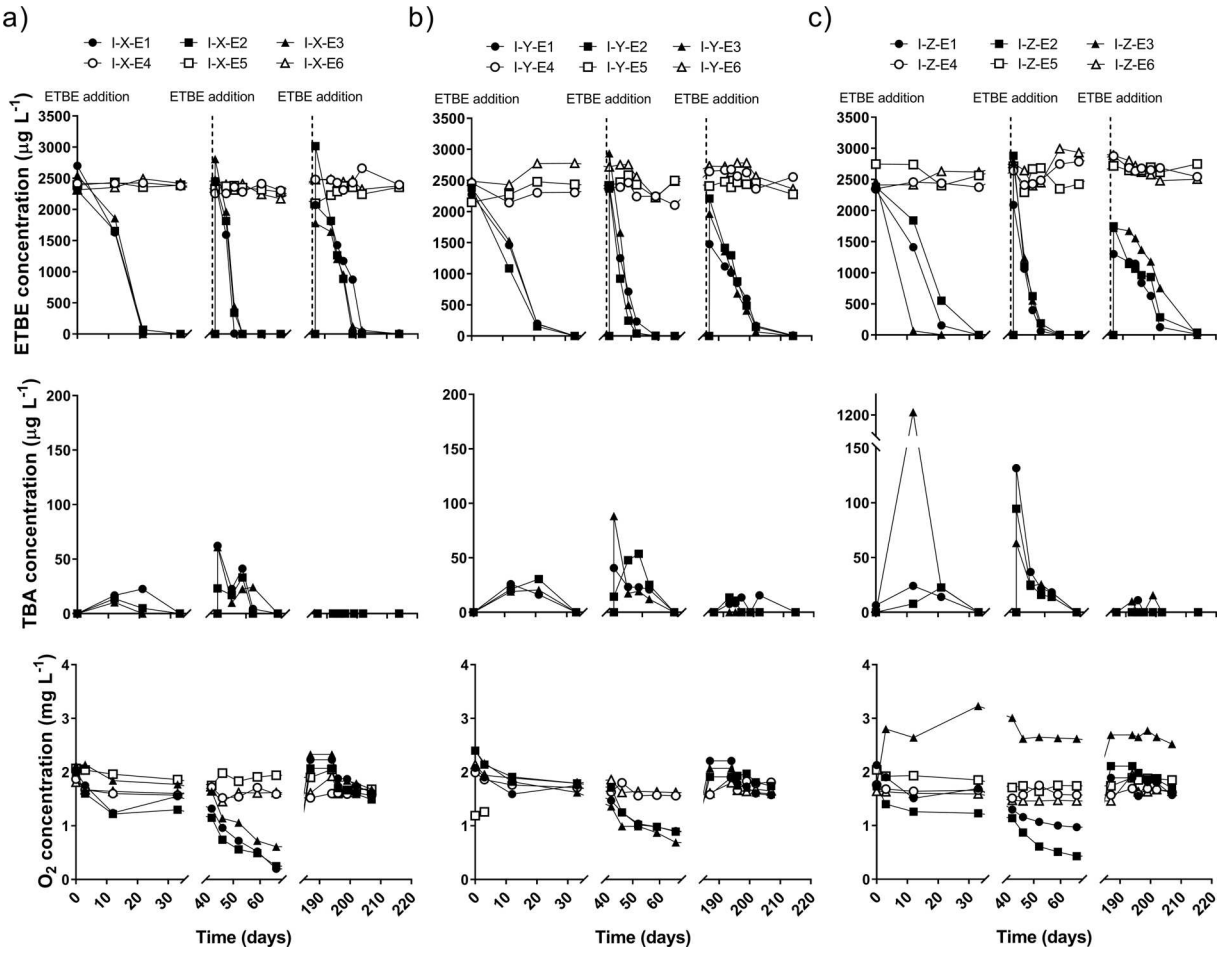

Fig. 3. ETBE, TBA and O_2 profiles for microcosms established using impacted (I) groundwater and aquifer material from a) depth 'x' (8–9 m), b) depth 'y' (9–10 m) and c) depth 'z' (13–14 m) located within the ETBE-impacted zone. Solid symbols are live microcosms and open symbols are sterile controls. ETBE was added three times to the microcosms, as indicated.

3.2. Quantification of GEO-degrading genes

qRT-PCR was used to quantify the *ethB* gene associated with ETBE biodegradation, the *mdpA* gene associated with MTBE biodegradation and 16S rRNA genes as a measure of cell number. Microbial cell counts of the planktonic and attached communities showed the presence of microbes in both matrices (Table S3, Figure S4), therefore a mixed groundwater-sediment sample was obtained for molecular analysis.

The *ethB* gene was below detection at the start of the experiment for microcosms established with inoculum from location N. After addition and subsequent biodegradation of ETBE, 10^5-10^6 copies g^{-1} sediment *ethB* were detected in microcosms N-X-E and 10^7 – 10^8 copies g^{-1} sediment in microcosms N-Z-E. Although the *ethB* copy numbers were highly responsive to ETBE addition, total microbial cell numbers, as estimated from 16S rRNA copy number, remained relatively constant at $\sim 10^5$ copies g^{-1} in N-X-E and $\sim 5 \times 10^8$ copies g^{-1} in N-Z-E (Fig. 5). The *ethB* gene persisted in all microcosms once present, even after extended incubation in the absence of GEO ('starvation period'). The *mdpA* gene was not detected in microcosms constructed with inoculum from location N.

The *ethB* gene was detected in all microcosms established with inoculum from location I, at 10^6, 10^5 and 10^5 copies g^{-1} sediment for microcosms I-X-E, I-Y-E and I-Z-E, respectively (Fig. 5c–e). The initial addition of ETBE resulted in an increase in *ethB* copy number in all microcosms ($>$ 100-fold), with further increases after the second addition of ETBE ($> 10^7$ copies g^{-1} sediment for all microcosms). The *ethB* gene remained during the starvation period. Microbial cell numbers remained constant at 10^9, 10^7 and 10^8 gene copies g^{-1} sediment for depths 'x', 'y' and 'z', respectively. The *mdpA* gene was detected only in bottles from depth 'y' (I-Y-E). The gene was initially detected before the first ETBE amendment ($\sim 10^4$ gene copies), increasing to $\sim 10^5$ copies g^{-1} sediment after the second ETBE addition. The gene was detected in all three replicates after two ETBE amendments, but only detectable thereafter in two of the replicates (Figure S5).

In microcosms amended with ETBE and MTBE the *ethB* gene was below the detection limit for location N microcosms but increased after exposure to ETBE and MTBE ($> 10^4$ *ethB* gene copies). In location I microcosms the *ethB* gene was above detection limits at the first sampling point and increased further after the first ETBE addition. Further additions of both ETBE and MTBE to both sets of microcosms resulted in an increase in the *ethB* gene copy numbers, which persisted even after the starvation period (Fig. 6). Microbial cell numbers remained constant for both sets of microcosms at $\sim 10^5$ and $\sim 10^9$ 16S rRNA gene copies g^{-1} sediment for location N and I, respectively. The *mdpA* gene was not detected in any microcosm bottles amended with both ETBE and MTBE.

3.3. Microbial community analysis via 16S rRNA sequencing

Microbial community composition was determined before and after GEO additions to microcosms. Fig. 7 shows the relative abundance of OTUs in each microcosm at the Class taxonomic levels, the predicted number of OTUs (Chao index) and the Shannon diversity index.

Microcosms inoculated with material from location I were

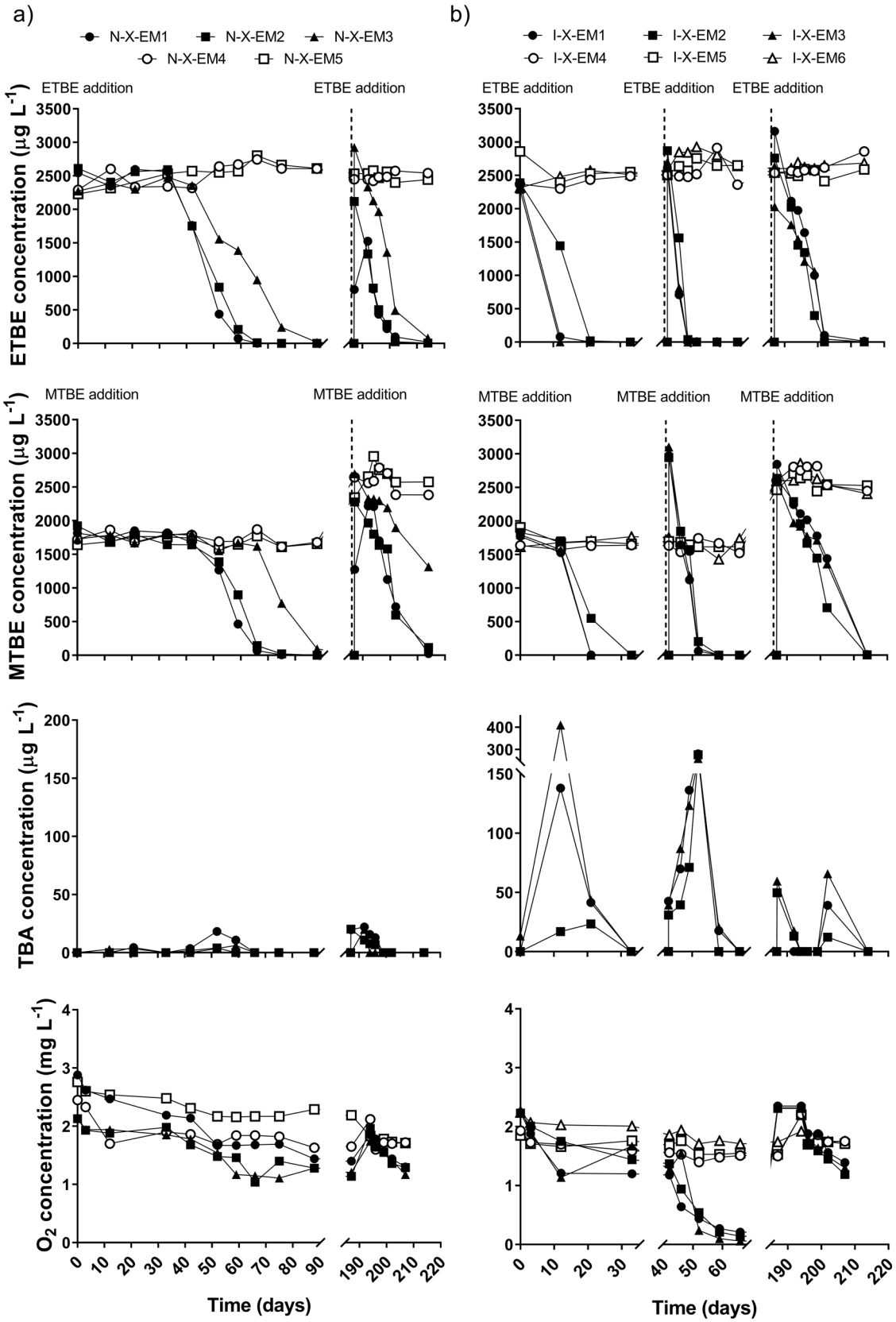

Fig. 4. ETBE, MTBE, TBA and O_2 profiles for microcosms established with aquifer material from depth 'x' (8–9 m) from a) non-impacted well, located upgradient of the ETBE-impacted zone, or b) impacted well, located within the ETBE-impacted zone. Solid symbols are live microcosms and open symbols are sterile controls. Two additions of ETBE and MTBE were made to well N microcosms and three additions of ETBE and MTBE were made to well I microcosms.

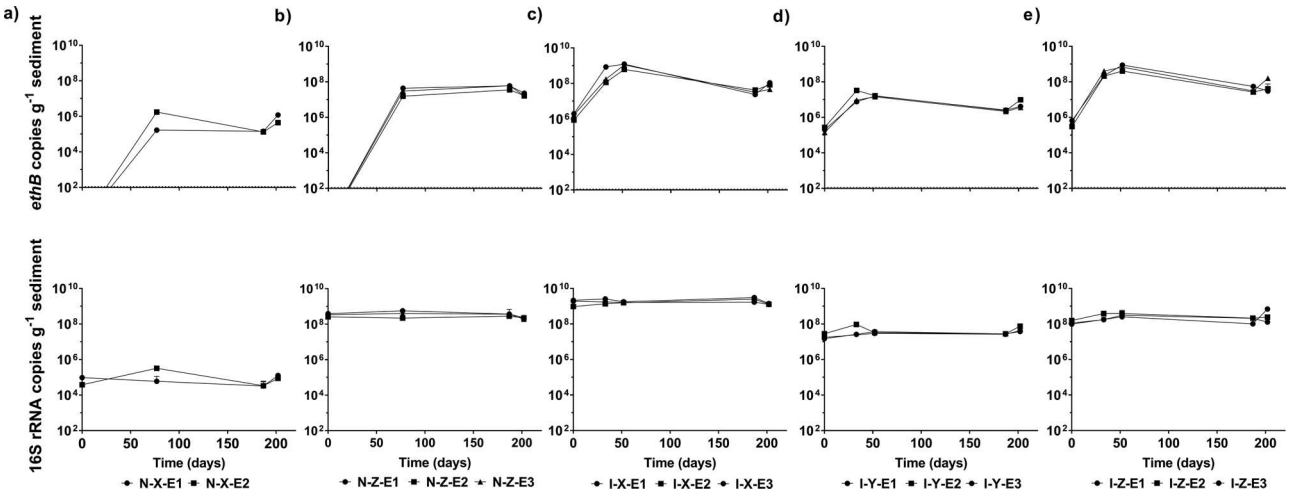

Fig. 5. *ethB* and 16S rRNA gene copy numbers for microcosms established using groundwater and aquifer material from a) depth 'x' (8–9 m) and b) 'z' (13–14 m), located upgradient of the ETBE-impacted zone (N), and groundwater and aquifer material from depths c) 'x' (8–9 m), d) 'y' (9–10 m) and e) 'z' (13–14 m), located within the ETBE-impacted zone (I). ETBE was the sole carbon source.

dominated by Proteobacteria (alpha, beta, delta and gamma). At depths 'y' and 'z' there were significant numbers of Actinobacteria and Leptospirae. For location I 'x' microcosms inoculated with ETBE or ETBE and MTBE, there was little difference in the microbial composition between microcosms and relatively small changes over time at the class level. Microcosms inoculated with material from location N 'z' were broadly similar to those from location I 'z', but microcosms from location N 'x' were dominated by betaproteobacteria, with gammaproteobacteria much reduced.

An estimation of the total numbers of taxa in the samples (rarefied for equal sampling depth) using the Chao1 index gave values of 3500–4000 in location I microcosms but lower numbers (2000–2500) in

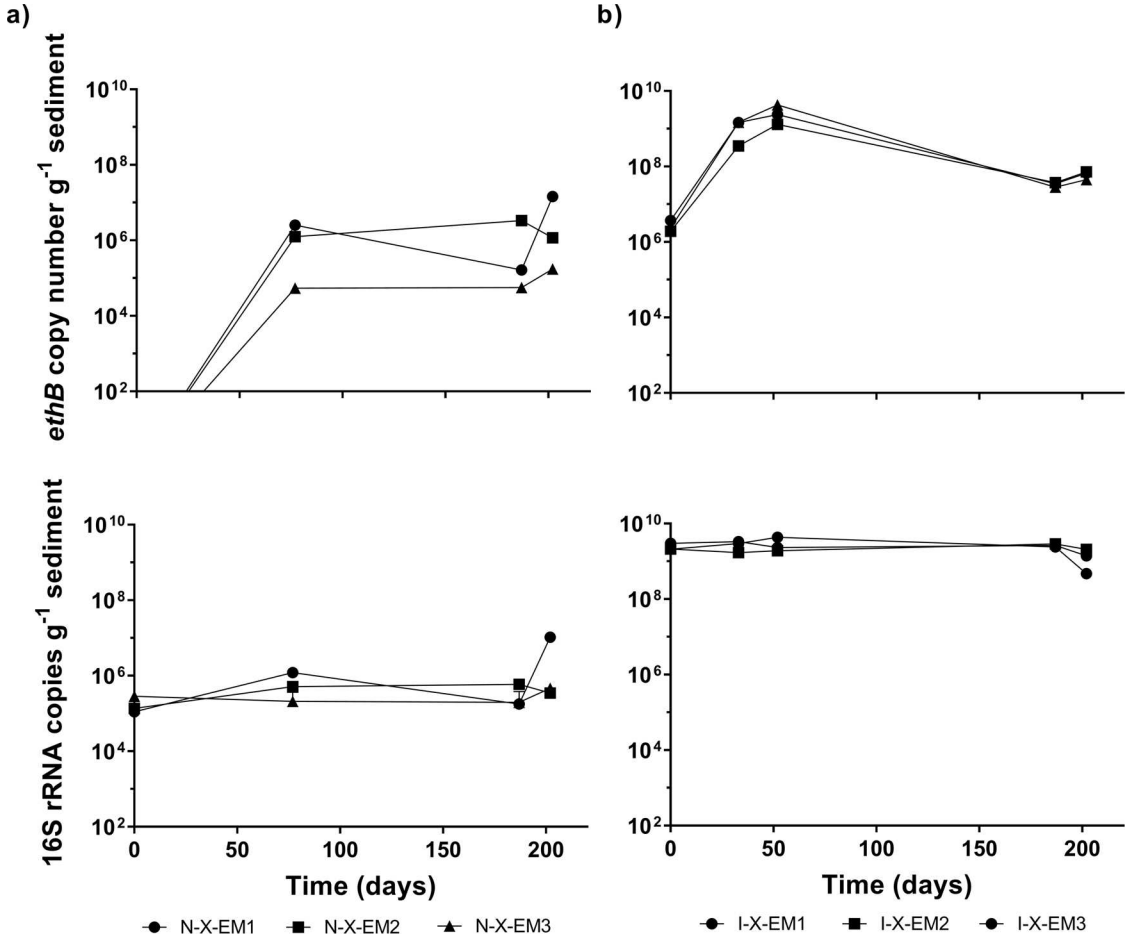

Fig. 6. *ethB* and 16S rRNA gene copy numbers for microcosms established using a) groundwater and aquifer material from depth 'x' (8–9 m), located upgradient of the ETBE-impacted zone (N), and b) groundwater and aquifer material from depth 'x' (8–9 m), located within the ETBE-impacted zone (I). Both ETBE and MTBE were added as carbon sources.

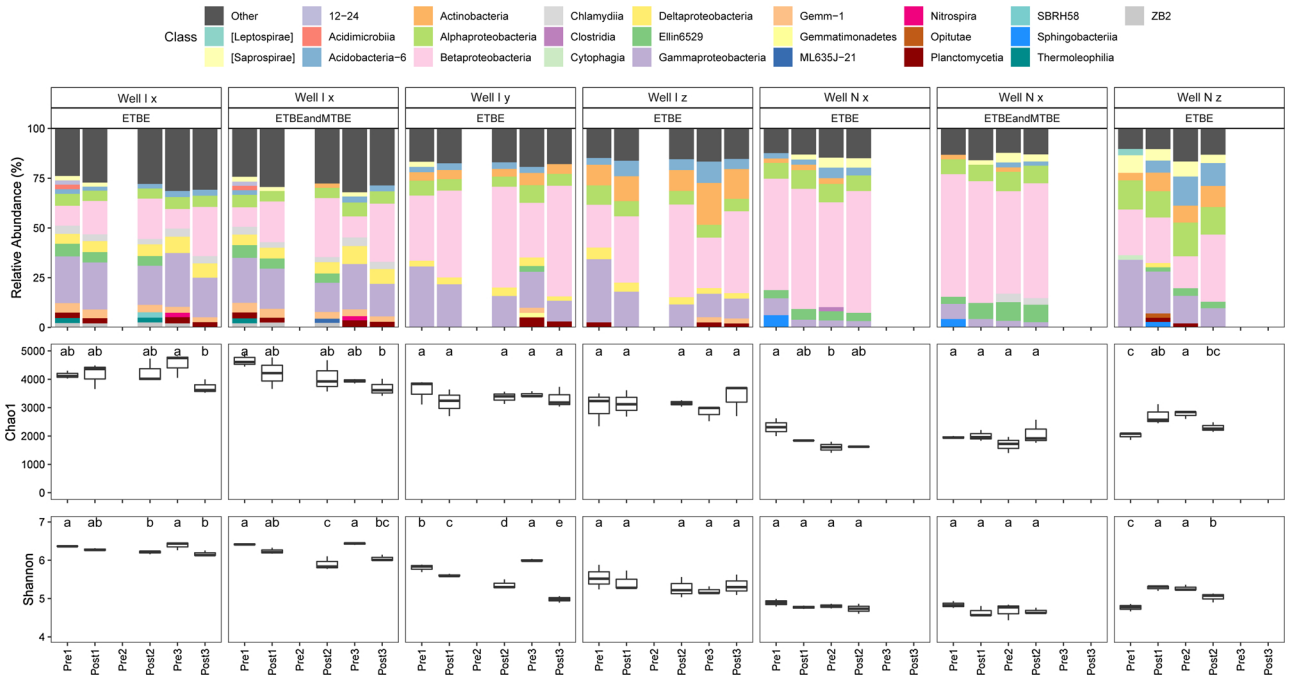

Fig. 7. a) Relative abundance of OTUs at the class level. Classes with a relative abundance of less than 1% have been categorised as 'Other' for clarity b) Chao1 and c) Shannon diversity indices. Pre/Post refer to time points immediately prior to addition of GEO and after the GEO had been metabolised. The extent of the boxes shows the interquartile range and the vertical bars the largest value within 1.5 times of the 25th and 75th interquartile percentile. Differences between timepoints within a microcosm are shown as letters – samples that share a letter were not statistically significantly different.

location N microcosms. The Shannon diversity index of location I microcosms was also higher (6–7) than location N (~5). Statistical analysis of these indices showed that these differences were highly significant ($p < 0.001$). The Shannon index in location I 'x' and 'y' microcosms was also affected by GEO addition, with the diversity falling after substrate addition.

Principal components analysis (PCA) of the microbial communities is shown in Fig. 8. Permanova analysis showed that all the communities in microcosms established from the two locations differed from each other ($p = 0.021$, ignoring the time of sampling) but that there was no difference between microcosms where ETBE only, or ETBE with MTBE, had been added ($p > 0.05$). In each case the addition of GEO, either as a single substrate or in combination, resulted in shifts in the microbial populations, although the changes were greatest after the initial addition (i.e. Pre1 vs Post1).

We hypothesised that GEO-responsive OTUs would increase in relative abundance after the addition of GEO. Therefore, a statistical analysis was performed to identify OTUs whose relative abundance differed before (Pre) and after (Post) each GEO addition. In total, 269 OTUs showed a difference in at least one comparison, with 109 showing

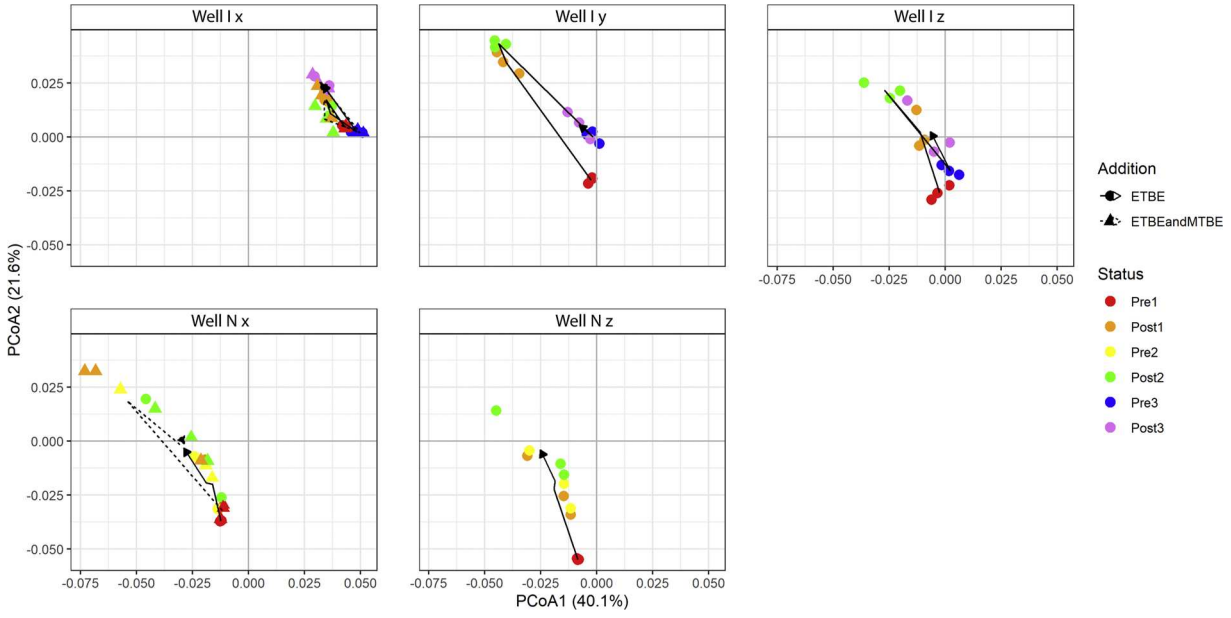

Fig. 8. Principal components analysis using weighted Unifrac distances of microcosms following additions of GEO (ETBE only or ETBE and MTBE). Microcosms are shown separately for clarity but are displayed on the same scales. Samples are colour-coded by time of incubation prior to (pre) and after (post) GEO addition with lines joining sample centroids.

differences in 2 comparisons or more. Fig. 9 shows the relative abundance and fold-changes (Pre/Post) for these OTUs.

Many OTUs increased relative abundance after the addition of GEO. In microcosms established using material from the non-impacted well N, the relative abundance of 128 OTUs increased upon the addition of ETBE, compared with 57 from the ETBE-impacted well I, with 22 OTUs common to both treatments (Figure S6a). In microcosms established from Well N, more OTUs increased in the shallower depth 'x' (72) compared to depth 'z' (43), with 16 in common (Figure S6b). Microcosms from Well I, depths 'x', 'y' and 'z' shared 10 OTUs that responded (Figure S6d). Of these OTUs, members of the Comamonadaceae family, in particular, increased in relative abundance, which were found in both location N and I microcosms and at all depths (Table 4). Many GEO-responsive OTUs in this family (33) were common to location N and I, found at all depths in location I (10) and to additions of ETBE only or combined ETBE and MTBE (11 and 12 for location N and I, respectively), reaching high relative abundances after GEO addition; 5 OTUs had relative abundances of 5% or more, with OTU#104281 reaching a relative abundance of 22.6%. Whilst the Comamonadaceae were numerically abundant, OTUs in 21 other Families also responded to GEO additions, particularly in microcosms established with inocula from location N. The most common of these were members of the beta and gamma proteobacteriaceae, Caulobacteraceae, Elusimicrobiales, Gemm-1 sp, Hyphomicrobiaceae, iii1-15 sp, Myxococcales sp, Sphingobacteriales sp and ZB2 sp – members of which were often also found in location I microcosms.

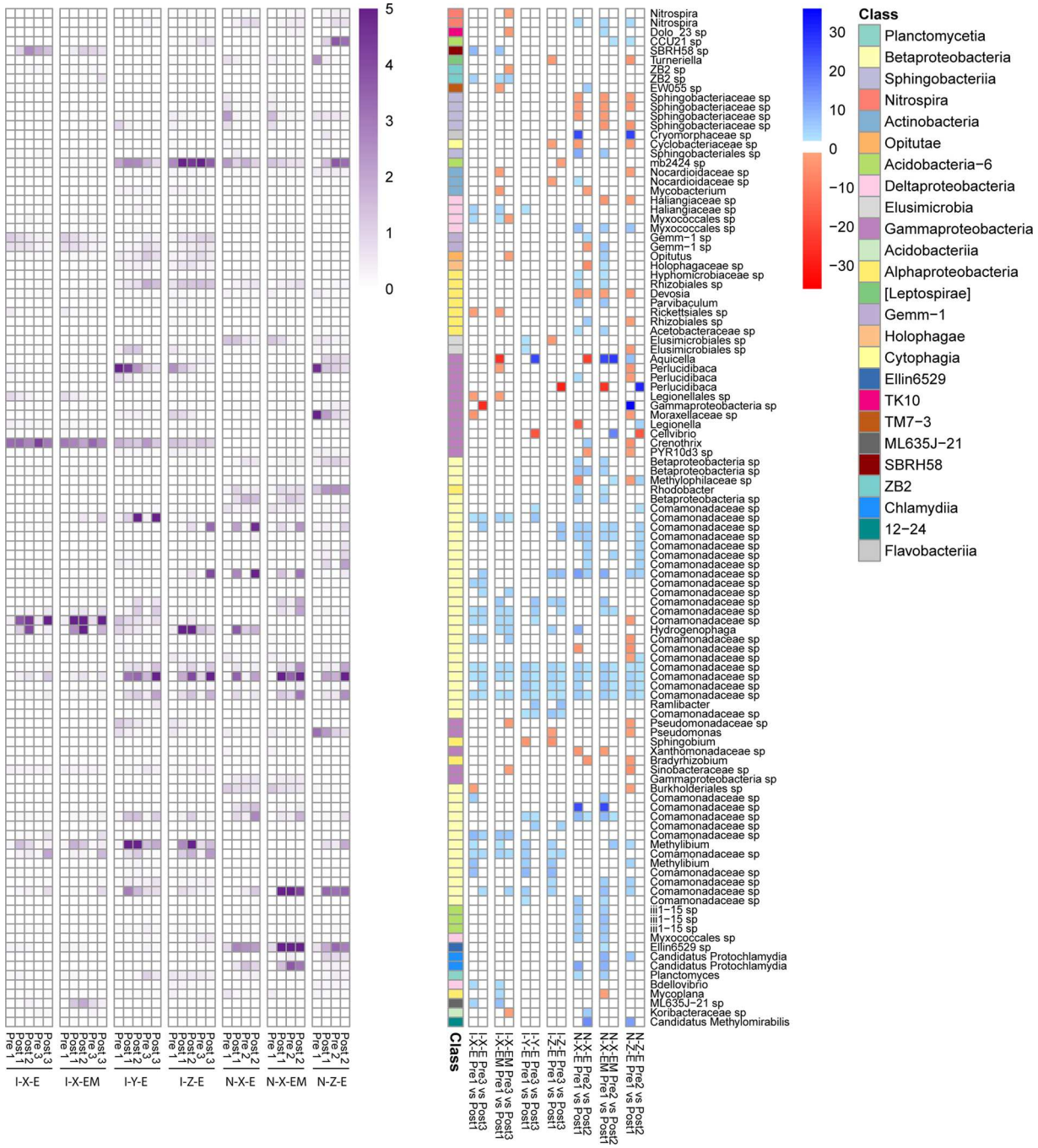

Fig. 9. Relative abundance (%) of OTUs in each microcosm. If the relative abundance exceeded 5%, values are displayed at 5% for clarity. Fold-changes for each comparison are shown before and after each GEO addition. OTUs have been organised by rows according to phylogeny.

Table 4
The number of OTUs at the Family taxonomic level that increased significantly between treatments. Families with 1 or 2 responses only have been omitted for clarity.

Microcosm	I	I	I	I	I	I	I	I	N	N	N	N	N	N
Depth	x	x	x	x	y	y	z	z	x	x	x	x	z	z
GEO addition	E	E	EM	EM	E	E	E	E	E	E	E v EM	E v EM	E	E
Time	Pre1vPost1	Pre3vPost3	Pre1vPost1	Pre3vPost3	Pre1vPost1	Pre3vPost3	Pre1vPost1	Pre3vPost3	Pre1vPost1	Pre2vPost2	Pre1vPost1	Pre2vPost2	Pre1vPost1	Pre2vPost2
Family														
Betaproteobacteria sp									8	1	4		1	
Caulobacteraceae			2								1	1	1	
CCU21 sp										1		1	1	
Comamonadaceae	15	15	11	12	13	14	15	15	13	1	15	1	22	12
Coxiellaceae			1			1	1			1	1	1	2	
Ellin6529 sp									2		1	1		
Elusimicrobiales sp					3		1						1	
Gammaproteobacteria sp		1	1						1		1		1	
Gemm-1 sp							3		1	2	3			
Haliangiaceae	1		1		1						1		3	
Hyphomicrobiaceae									3	2	3		2	
iii1-15 sp									3	2	4			
Legionellaceae									1	2	1			1
mb2424							1	1					3	
Myxococcales sp	1		1	1					2		3		2	
Nitrospiraceae				1					1		1		2	
Parachlamydiaceae									2		2		1	
Planctomycetaceae									2		2		2	
Rhizobiales sp									2	1	3		4	
Rhodobacteraceae									1		2		1	
Sphingobacteriales sp					2				1		1		2	
ZB2 sp	1		2	2				1						

Direct comparisons between microcosms with ETBE only or combined ETBE and MTBE additions were made for microcosms I-X-EM and N-X-EM. Both Well N and I microcosms shared OTUs that increased in relative abundance, with a greater number of OTUs increasing in microcosms from Well N than for Well I (Figure S6c, e). OTUs that increased in abundance only in response to ETBE and MTBE additions are likely to include those that could only utilise MTBE or a specific metabolite of this GEO. OTUs that responded only to ETBE additions, but not combined ETBE and MTBE, will include organisms whose growth was inhibited by MTBE or who are out-competed by other community members. Representatives for each of these possibilities were found in the Comamonadaceae, indicating broad metabolic diversity in this Family. In contrast, OTUs in the Gemm-1 and Caulobacteraceae Families and some Rhizobiales sp were found only when MTBE was included, indicating metabolic specificity.

4. Discussion

4.1. Biodegradation behaviour and relationships between GEO, TBA and dissolved oxygen

Previous exposure to a GEO source was the strongest factor influencing ETBE biodegradation. Generally, ETBE biodegradation occurred after a longer lag and at a slower rate in locations with no known history of exposure to ETBE, compared with locations impacted by the GEO plume. Aquifer depth had less influence, with differences in lags and biodegradation rates being greatest between the first ETBE addition in the non-impacted location, depth 'x' and 'z'. Further additions of ETBE reduced the duration of the lag period and increased biodegradation rates in both non-impacted and impacted locations. This behaviour is consistent with a progressive enrichment of ETBE-biodegrading microorganisms in the consortia. Considering the respective time scales (days-weeks) of the lag phases, this presumably occurs for non-impacted locations by induction of requisite enzyme systems in native microorganisms and sufficient biomass growth to effect degradation (Alexander, 1999; Chapelle, 2001; Shah et al., 2009). For impacted locations ETBE biodegradation is likely to be initiated quickly upon re-exposure by a standing population of ETBE-degrading microorganisms adapted to the plume conditions through previous exposure. These changes in the relative abundance of ETBE-degrading organisms take place without significant changes in total microbial cell numbers (as measured by 16S rRNA gene copy number), and therefore other nutrients are likely to limit total cell numbers.

These observations are supported by *ethB* gene numbers which were below detection limits in the microbial community of the location N microcosms prior to amendment with ETBE or ETBE and MTBE (suggesting very low numbers of ETBE-degraders). It contrasts with the abundance of this gene in the corresponding microcosms established with inoculum from location I, which confirms an established community of ETBE-degraders at the ETBE-impacted location. After the addition of ETBE, the *ethB* gene copy number increased over a 100-fold for location I microcosms and over 10,000-fold for location N microcosms, revealing the rapid increase in relative abundance of ETBE-degraders in the respective consortia. The increase in *ethB* gene abundance after re-addition of ETBE to the microcosms likely reflects further increases in relative abundance of ETBE-degrading microorganisms, as would occur after renewed exposure at the field site. After these initial increases, the relative abundance of *ethB* gene-containing microorganisms remained high throughout the experiment with little decrease during the starvation period between ETBE additions. In contrast to this study, Fayolle-Guichard et al. (2012) observed a rapid decrease in the abundance of *ethB* gene-containing microorganisms over 20 days in the absence of ETBE when in batch conditions. In the latter study three organisms (*Rhodococcus wratislaviensis* IFP 2016, *R. aetherivorans* IFP 2017 and *Aquincola tertiaricarbonis* IFP 2003) were selected for use in a pilot plant fed with ETBE and SP98 gasoline, wherein the rapid decrease of the *ethB* gene suggests that these strains require continual feeding to maintain high cell numbers. The persistence of the *ethB* gene in our study indicates that the potential for ETBE biodegradation is retained via a population of ETBE-degraders in the microbial community during periods of starvation and is quickly re-established with repeated exposure to ETBE.

Analysis of TBA behaviour in the respective experiments offers further insight on the development of the microbial community in these systems. Very few microorganisms have been identified with the ability to fully mineralise ETBE and in many cases ETBE biodegradation appears to be facilitated by commensal interactions between different community members which degrade the parent compound and intermediate metabolite separately (Le Digabel et al., 2013). TBA biodegradation is considered to be rate limiting when ETBE biodegradation is rapid (Le Digabel et al., 2014). No TBA was detected in location N 'x' microcosms in the ETBE-only systems, whereas there was transient accumulation of TBA in the 'z' microcosms (Fig. 2). A similar feature is evident in the location N 'x' microcosms amended with ETBE and MTBE, where there was very little accumulation of TBA after both additions of the GEO (Fig. 4a). This could indicate that depth 'x' had an established community of active TBA-degraders, whereas a slower developing community of TBA-degraders existed at depth 'z' at this location. TBA accumulated to a lesser extent with the second addition of ETBE in the ETBE-only systems, suggesting an enrichment of TBA-degrading microorganisms within the microbial community. In contrast, TBA generally accumulated at lower concentration in the ETBE-only microcosms from location I (Fig. 3). However, a higher TBA concentration was correlated with relative rapid ETBE biodegradation after the first ETBE addition in microcosm I-Z-E3 and the second ETBE addition in replicates from all three depths at this location in the ETBE-only systems (Fig. 3). In microcosms from location I amended with both ETBE and MTBE, TBA consistently accumulated after each addition of GEO, due to ETBE and MTBE biodegradation (Fig. 4b). As with the corresponding ETBE-only system (Fig. 3) TBA accumulation in the ETBE- and MTBE-amended systems was correlated with GEO biodegradation rate, particularly evident for ETBE. This behaviour also corresponded with more rapid consumption of dissolved oxygen, which did not occur at lower ETBE or MTBE biodegradation rates or TBA production. It is particularly striking for impacted location I microcosms amended with ETBE (Fig. 3) and both ETBE and MTBE (Fig. 4). This implies the presence of an established population of TBA-degraders in the aquifer microbial community at the ETBE-impacted location. However, TBA metabolism is clearly the rate-limiting step in ETBE and MTBE biodegradation when the latter is rapid.

4.2. Development of microbial community and ETBE biodegradation potential

PCA revealed that location N and I differed in their initial microbial community composition, with slight differences between depths. Microbial community analysis showed that location N 'x' was dominated by betaproteobacteria and after the ETBE addition showed a greater number of organisms that increased in abundance, whereas the 'z' microbial community was less dominated by this group. For location I, PCA also revealed differences in the microbial community composition between aquifer depths, especially at 'x', but regardless of the starting communities, organisms belonging to the Comamonadaceae family were the most common responder, i.e. they increased in relative abundance after each GEO addition. However, there were notable differences in the microbial communities; location I 'y' and 'z' had significant numbers of Actinobacteria and Leptospirae, but not at depth 'x'. Organisms belonging to the Phylum Actinobacteria have been shown to degrade ETBE to TBA (Le Digabel et al., 2014), and include *Rhodococcus* spp.; many of these organisms have been isolated from ETBE release sites and can metabolise ETBE (Malandain et al., 2010; Le Digabel et al., 2014). Phylogenetic variation in the responsive organisms at different

depths, if assumed to be ETBE-degraders, could further explain the difference in microcosm biodegradation rates; closely related ETBE-degraders have been shown to utilise ETBE at different rates (1110 – 3509 μmol $g^{-1} h^{-1}$) (Müller et al., 2008; Malandain et al., 2010). Furthermore, the detection of the *mdpA* gene in location I 'y' only confirms that these aquifer depths have different microbial communities. While the enzyme encoded by the *mdpA* gene has no known activity towards ETBE (Schmidt et al., 2008), organisms containing this gene, such as *Methylibium petroleiphilum* PM1, are also known to degrade TBA (Joshi et al., 2016).

As GEO was the sole carbon source in the microcosms, it was hypothesised that the relative abundance of GEO-degrading microbes would increase, leading to greater similarity in the microbial community composition, regardless of exposure history or aquifer depth. The qRT-PCR analysis showed that *ethB* gene-containing organisms increased in abundance in all locations and became dominant once exposed to ETBE, yet the 16S rRNA gene numbers remained stable. The stability in bacterial numbers suggests a nutrient limitation, as found in oligotrophic environments. This is most likely a result of PO_4 limitation, which was below detection in the groundwater (data not shown). The stability in bacterial cell numbers was further confirmed by live/dead counting of planktonic cells before and after GEO addition. Whilst the planktonic community represents only a portion of the total microcosm community, this analysis further confirmed that cell numbers did not change and that most cells were live (Table S3). It is thought that most organisms in aquifers are attached to sediment (Griebler and Lueders, 2009) and to confirm an attached microbial community in the aquifer, fluorescence microscopy images of sediment grains were obtained. While it is difficult to quantify bacterial numbers with this technique, a significant attached community was confirmed (Figure S4). Furthermore, GEO-degrading organisms have been shown to attach to surfaces in bioreactors (Hicks et al., 2014; Alfonso-Gordillo et al., 2016; Kharoune et al., 2002; Purswani et al., 2011; Pannier et al., 2010), suggesting that these organisms would attach to the aquifer material. In some microcosms the ratio of *ethB*:16S rRNA was > 1. To the best of our knowledge no complete genome sequence of an ETBE degrader has been reported and therefore the number of *ethB* genes per genome is unknown, but is assumed as one gene copy. However, our data suggests that this may not be true for all *ethB* gene-containing organisms.

Representatives of the Comamonadaceae family were the most commonly identified organisms that increased in abundance after ETBE additions in all microcosms, regardless of exposure history or aquifer depth. Organisms such as strain L108, T29 and PM1 belong to the Comamonadaceae and have been reported to degrade both ETBE and TBA (Rohwerder et al., 2006) or TBA only (Szabó et al., 2015). The presence of Comamonadaceae has also been reported in a batch-fed bioreactor, established with ETBE-contaminated groundwater (van der Waals et al., 2019). A possible explanation for closely related Comamonadaceae responding to ETBE additions in all microcosms is that the *ethB* gene cluster is flanked by identical transposons (Chauvaux et al., 2001), enabling the transfer of this gene cluster as a hairpin structure to closely related organisms. Five OTUs reached a relative abundance of 5% or more, with OTU#104281 reaching over 20%. This corresponded with the large increase in *eth*B gene-containing organisms, as measured by qRT-PCR. While members of the Comamonadaceae increased in relative abundance in all microcosms, a greater number of responders were evident in location N microcosms, suggesting an adapting community, whereas an acclimated ETBE-degrading community was already present in location I microcosms, as confirmed by qRT-PCR.

4.3. Biodegradation of MTBE and ETBE as co-substrates

The biodegradation of MTBE and ETBE as co-substrates was examined by comparing these systems with those exposed to ETBE only. In microcosms containing both oxygenates ETBE was biodegraded before MTBE (Fig. 4) and MTBE biodegradation rates were highest after most ETBE was biodegraded (Table 3). The third addition of GEO to microcosm I-X-EM resulted in two peak concentrations of TBA, corresponding to the sequential biodegradation of ETBE followed by MTBE. These data suggest that either two enzyme systems are responsible for separate ETBE and MTBE biodegradation or that one enzyme system with broad substrate capability biodegraded both ETBE and MTBE, with preference for ETBE. The *mdpA* gene was not detected in ETBE- and MTBE-amended microcosms, confirming that the known route for MTBE biodegradation was not present within the population. However, the *ethB* gene was detected and increased with exposure to GEO. Unlike ETBE, MTBE is not known to induce *ethB* gene expression (Malandain et al., 2010) and the cytochrome P450 encoded by this gene has comparable activity towards ETBE and MTBE when provided as single substrates (Müller et al., 2008; Schuster et al., 2013), but in a mixture ETBE is preferentially degraded. Therefore, the presence of ETBE would induce the expression of the *ethB* gene (via interaction with the *eth* operon regulator *ethR*), resulting in the biodegradation of both ETBE and MTBE. Given the known route for MTBE biodegradation was not present and that the *ethB* cytochrome has broad GEO activity, the data from this study suggests that the *ethB* gene was responsible for the biodegradation of both GEO.

The presence of MTBE did not affect ETBE biodegradation rates. As the only detected route of GEO biodegradation in the microcosms was via *ethB*, the presence of MTBE would not increase the expression of this gene as it is not known to interact with the eth operon regulator (*ethR*). While ETBE biodegradation rates were increased for the second GEO addition in location I microcosms, the biodegradation rates are otherwise comparable to microcosms amended with ETBE only. Community analysis showed that OTUs belonging to the Gemm-1 and Caulobacteraceae Families and Rhizobiales sp were present only when MTBE was added, suggesting that these organisms possess the metabolic capability for biodegradation of ETBE or intermediate metabolites of ETBE and MTBE biodegradation, such as TBA. As in the microcosms amended with ETBE only, Comamonadaceae were also identified when MTBE was present.

5. Conclusions

This study has shown the potential for aerobic ETBE biodegradation in groundwater when oxygen is not limiting, with this being the most commonly reported environmental condition under which ETBE biodegradation occurs. A few examples of anaerobic ETBE biodegradation have been reported and these differ significantly in their behaviour, such as having longer lags preceding biodegradation and reduced biodegradation rates, compared with aerobic systems.

Exposure to ETBE leads to the development of microbial communities that are enriched in ETBE-degraders, specifically in organisms containing the *eth* gene cluster. This exposure leads to reduced lags preceding biodegradation and rapid ETBE biodegradation upon re-exposure, with persistence of the ETBE-degrading organisms for extended periods once ETBE has been consumed. This study was conducted in essentially a nutrient limited oligotrophic environment, but with carbon available to the organisms that can degrade ETBE and its metabolites. Therefore, overall cell numbers do not increase, whereas the proportion of ETBE-degraders does. These environmental characteristics are likely to be typical of many ETBE-impacted sites where groundwater experiences an influx of xenobiotic organic chemicals but remains nutrient (e.g. nitrogen or phosphate) limited. Members of the Comamonadaceae family were enriched in the studied systems. Organisms belonging to this family have been reported in the literature as ETBE-degraders, but do not reach high abundance. Therefore, we propose that it is the presence of the ETBE-degrading genes that drives changes in the microbial community, rather than specific taxonomic groups. This is not unexpected given the known mobility of the *eth* gene cluster. This property could be exploited at different sites as the *eth* gene cluster could be acquired by other taxonomic groups that are

adapted to the local environmental conditions. The experimental approach adopted in this study may provide a useful basis to support the assessment of GEO biodegradation potential in groundwater at gasoline-impacted sites. The research underpinning this study will be summarised in a project report by Concawe in due course (www.concawe.eu).

Declaration of interests

None.

CRediT authorship contribution statement

H.C.G. Nicholls: Methodology, Validation, Formal analysis, Investigation, Data curation, Writing - original draft, Writing - review & editing, Visualization. **H.E.H. Mallinson:** Methodology, Validation, Formal analysis, Investigation, Data curation. **S.A. Rolfe:** Conceptualization, Methodology, Formal analysis, Data curation, Writing - original draft, Writing - review & editing, Visualization, Supervision. **M. Hjort:** Project administration, Resources. **M.J. Spence:** Conceptualization, Project administration, Methodology, Resources. **S.F. Thornton:** Conceptualization, Methodology, Writing - original draft, Writing - review & editing, Supervision, Funding acquisition.

Acknowledgements

This research was completed within a project funded by Concawe (www.concawe.eu), which is the scientific division of the European Petroleum Refiners Association, under contract 201601270. The authors acknowledge the support and advice of Birgitta Beuthe, Matthijs Bonte, Sandrine Demeure, Martyn Dunk, Céline Pisano and Jonathan Smith from the Concawe Soil and Groundwater Task Force (STF33) in the preparation of the manuscript.

Appendix A. Supplementary data

Supplementary material related to this article can be found, in the online version, at doi:https://doi.org/10.1016/j.jhazmat.2020.122022.

References

Alexander, M., 1999. Biodegradation and Bioremediation. Academic Press, San Diego, Ca.
Alfonso-Gordillo, G., Flores-Ortiz, C.M., Morales-Barrera, L., Cristiani-Urbina, E., 2016. Biodegradation of methyl tertiary butyl ether (MTBE) by a microbial consortium in a continuous up-flow packed-bed biofilm reactor: kinetic study, metabolite identification and toxicity bioassays. PLoS One 11, e0167494. https://doi.org/10.1371/journal.pone.0167494.
Blume, E., Bischoff, M., Reichert, J.M., Moorman, T., Konopka, A., Turco, R.F., 2002. Surface and subsurface microbial biomass, community structure and metabolic activity as a function of soil depth and season. Appl. Soil Ecol. 20, 171–181. https://doi.org/10.1016/S0929-1393(02)00025-2.
Bodenhausen, N., Horton, M.W., Bergelson, J., 2013. Bacterial communities associated with the leaves and the roots of *Arabidopsis thaliana*. PLoS One 8, e56329. https://doi.org/10.1371/journal.pone.0056329.
Bombach, P., Nägele, N., Rosell, M., Richnow, H.H., Fischer, A., 2015. Evaluation of ethyl *tert*-butyl ether biodegradation in a contaminated aquifer by compound-specific isotope analysis and *in situ* microcosms. J. Hazard. Mater. 286, 100–106. https://doi.org/10.1016/j.jhazmat.2014.12.028.
Caporaso, J.G., Bittinger, K., Bushman, F.D., DeSantis, T.Z., Andersen, G.L., Knight, R., 2010a. PyNAST: a flexible tool for aligning sequences to a template alignment. Bioinformatics 26, 266–267. https://doi.org/10.1093/bioinformatics/btp636.
Caporaso, J.G., Kuczynski, J., Stombaugh, J., Bittinger, K., Bushman, F.D., Costello, E.K., Fierer, N., Pẽa, A.G., Goodrich, J.K., Gordon, J.I., Huttley, G.A., Kelley, S.T., Knights, D., Koenig, J.E., Ley, R.E., Lozupone, C.A., McDonald, D., Muegge, B.D., Pirrung, M., Reeder, J., Sevinsky, J.R., Turnbaugh, P.J., Walters, W.A., Widmann, J., Yatsunenko, T., Zaneveld, J., Knight, R., 2010b. QIIME allows analysis of high-throughput community sequencing data. Nat. Methods 7, 335–336. https://doi.org/10.1038/nmeth.f.303.
Chapelle, F.H., 2001. Groundwater Microbiology and Geochemistry, 2nd ed. John Wiley and Sons, New York.
Chauvaux, S., Chevalier, F., Le Dantec, C., Fayolle, F., Miras, I., Kunst, F., Beguin, P., 2001. Cloning of a genetically unstable cytochrome P-450 gene cluster involved in degradation of the pollutant ethyl *tert*-butyl ether by *Rhodococcus ruber*. J. Bacteriol. 183, 6551–6557. https://doi.org/10.1128/JB.183.22.6551-6557.2001.
Davis, L.C., Erickson, L.E., 2004. A review of bioremediation and natural attenuation of MTBE. Environ. Prog. 23, 243–252. https://doi.org/10.1002/ep.10028.
Deeb, R.A., Scow, K.M., Alvarez-Cohen, L., 2000. Aerobic MTBE biodegradation: an examination of past studies, current challenges and future research directions. Biodegradation 11, 171–185. https://doi.org/10.1023/A:1011113320414.
Deeb, R.A., Hu, H.Y., Hanson, J.R., Scow, K.M., Alvarez-Cohen, L., 2001. Substrate interactions in BTEX and MTBE mixtures by an MTBE-degrading isolate. Environ. Sci. Technol. 35, 312–317. https://doi.org/10.1021/es001249j.
DeSantis, T.Z., Hugenholtz, P., Larsen, N., Rojas, M., Brodie, E.L., Keller, K., Huber, T., Dalevi, D., Hu, P., Andersen, G.L., 2006. Greengenes, a chimera-checked 16S rRNA gene database and workbench compatible with ARB. Appl. Environ. Microbiol. 72, 5069–5072. https://doi.org/10.1128/AEM.03006-05.
Edgar, R.C., 2010. Search and clustering orders of magnitude faster than BLAST. Bioinformatics 26, 2460–2461. https://doi.org/10.1093/bioinformatics/btq461.
Eilers, K.G., Debenport, S., Anderson, S., Fierer, N., 2012. Digging deeper to find unique microbial communities: the strong effect of depth on the structure of bacterial and archaeal communities in soil. Soil Biol. Biochem. 50, 58–65. https://doi.org/10.1016/j.soilbio.2012.03.011.
Environmental Protection Agency, 1997. Drinking Water Advisory: Consumer Acceptability Advice and Health Effects Analysis on Methyl Tertiary-Butyl Ether (MtBE). United States Envitonmental Protection Agency EPA 822-F-97-009.
Fayolle, F., Hernandez, G., Le Roux, F., Vandecasteele, J.P., 1998. Isolation of two aerobic bacterial strains that degrade efficiently ethyl *t*-butyl ether (ETBE). Biotechnol. Lett. 20, 283–286. https://doi.org/10.1023/A:1005390221856.
Fayolle, F., Vandecasteele, J.-P., Monot, F., 2001. Microbial degradation and fate in the environment of methyl *tert*-butyl ether and related fuel oxygenates. Appl. Microbiol. Biotechnol. 56, 339–349. https://doi.org/10.1007/s002530100647.
Fayolle-Guichard, F., Durand, J., Cheucle, M., Rosell, M., Michelland, R.J., Tracol, J.P., Le Roux, F., Grundman, G., Atteia, O., Richnow, H.H., Dumestre, A., Benoit, Y., 2012. Study of an aquifer contaminated by ethyl*tert*-butyl ether (ETBE): Site characterization and on-site bioremediation. J. Hazard. Mater. 201–202, 236–243. https://doi.org/10.1016/j.jhazmat.2011.11.074.
Feris, K.P., Hristova, K., Gebreyesus, B., Mackay, D., Scow, K.M., 2004. A shallow BTEX and MTBE contaminated aquifer supports a diverse microbial community. Microb. Ecol. 48, 589–600. https://doi.org/10.1007/s00248-004-0001-2.
Fiorenza, S., Rifai, H.S., 2003. Review of MTBE biodegradation and bioremediation. Bioremediat. J. 7, 1–35. https://doi.org/10.1080/713914240-243.
Franklin, R.B., Taylor, D.R., Mills, A.L., 1999. The distribution of microbial communities in anaerobic and aerobic zones of a shallow coastal plain aquifer. Microb. Ecol. 38, 377–386. https://doi.org/10.1007/s002489900179.
Griebler, C., Lueders, T., 2009. Microbial biodiversity in groundwater ecosystems. Freshw. Biol. 54, 649–677. https://doi.org/10.1111/j.1365-2427.2008.02013.x.
Hanson, J.R., Ackerman, C.E., Scow, K.M., 1999. Biodegradation of methyl *tert*-butyl ether by a bacterial pure culture. Appl. Environ. Microbiol. 65, 4788–4792.
Hernandez-Perez, G., Fayolle, F., Vandecasteele, J.P., 2001. Biodegradation of ethyl *t*-butyl ether (ETBE), methyl *t*-butyl ether (MTBE) and *t*-amyl methyl ether (TAME) by *Gordonia terrae*. Appl. Microbiol. Biotechnol. 55, 117–121. https://doi.org/10.1007/s002530000482.
Hicks, K.A., Drive, T.C., Boyle, S.L., Baker, J.M., 2014. Successful treatment of an MTBE-impacted aquifer using a bioreactor self-colonized by native aquifer bacteria. Biodegradation 25, 41–53. https://doi.org/10.1007/s10532-013-9639-0.Successful.
Hyman, M., 2013. Biodegradation of gasoline ether oxygenates. Curr. Opin. Biotechnol. 24, 443–450. https://doi.org/10.1016/j.copbio.2012.10.005.
Jechalke, S., Rosell, M., Martínez-Lavanchy, P.M., Pérez-Leiva, P., Rohwerder, T., Vogt, C., Richnow, H.H., 2011. Linking low-level stable isotope fractionation to expression of the cytochrome P450 monooxygenase-encoding ethB gene for elucidation of methyl *tert*-butyl ether biodegradation in aerated treatment pond systems. Appl. Environ. Microbiol. 77, 1086–1096. https://doi.org/10.1128/AEM.01698-10.
Joshi, G., Schmidt, R., Scow, K.M., Denison, M.S., Hristova, K.R., 2016. Effect of benzene and ethylbenzene on the transcription of methyl-*tert*-butyl ether degradation genes of Methylibium petroleiphilum PM1. Microbiology 162, 1563–1571. https://doi.org/10.1099/mic.0.000338.
Kharoune, M., Kharoune, L., Lebault, J.-M., Pauss, A., 2002. Aerobic degradation of ethyl-*tert* -butyl ether by a microbial consortium: selection and evaluation of biodegradation ability. Environ. Toxicol. Chem. 21, 2052–2058. https://doi.org/10.1002/etc.5620211007.
Klindworth, A., Pruesse, E., Schweer, T., Peplies, J., Quast, C., Horn, M., Glöckner, F.O., 2013. Evaluation of general 16S ribosomal RNA gene PCR primers for classical and next-generation sequencing-based diversity studies. Nucleic Acids Res. 41, 1–11. https://doi.org/10.1093/nar/gks808.
Kulkarni, P., King, D., Moran, K., McHugh, T., 2018. Survey of Natural Attenuation of Petroleum Hydrocarbon Plumes in Groundwater in Europe. Concawe Report 10/18.
Le Digabel, Y., Demanèche, S., Benoit, Y., Vogel, T.M., Fayolle-Guichard, F., 2013. Ethyl *tert*-butyl ether (ETBE) biodegradation by a syntrophic association of *Rhodococcus* sp. IFP 2042 and *Bradyrhizobium* sp. IFP 2049 isolated from a polluted aquifer. Appl. Microbiol. Biotechnol. 97, 10531–10539. https://doi.org/10.1007/s00253-013-4803-3.
Le Digabel, Y., Demanèche, S., Benoit, Y., Fayolle-Guichard, F., Vogel, T.M., 2014. Ethyl *tert*-butyl ether (ETBE)-degrading microbial communities in enrichments from polluted environments. J. Hazard. Mater. 279, 502–510. https://doi.org/10.1016/j.jhazmat.2014.07.013.
Lima, G., da, P., Meyer, J.R., Khosla, K., Dunfield, K.E., Parker, B.L., 2018. Spatial variability of microbial communities in a fractured sedimentary rock matrix impacted by a mixed organics plume. J. Contam. Hydrol. 218, 110–119. https://doi.org/10.1016/j.jconhyd.2018.10.001.

Love, M.I., Huber, W., Anders, S., 2014. Moderated estimation of fold change and dispersion for RNA-seq data with DESeq2. Genome Biol. 15 (550), 1–21. https://doi.org/10.1186/s13059-014-0550-8.

Lozupone, C., Lladser, M.E., Knights, D., Stombaugh, J., Knight, R., 2011. UniFrac: an effective distance metric for microbial community comparison. ISME J. 5, 169–172. https://doi.org/10.1038/ismej.2010.133.

Malandain, C., Fayolle-Guichard, F., Vogel, T.M., 2010. Cytochromes P450-mediated degradation of fuel oxygenates by environmental isolates. FEMS Microbiol. Ecol. 72, 289–296. https://doi.org/10.1111/j.1574-6941.2010.00847.x.

Martinez Arbizu, P., 2019. pairwiseAdonis: Pairwise Multilevel Comparison Using Adonis. R Package Version 0.3.

McMurdie, P.J., Holmes, S., 2013. Phyloseq: an R package for reproducible interactive analysis and graphics of microbiome census data. PLoS One 8, e61217. https://doi.org/10.1371/journal.pone.0061217.

Medihala, P.G., Lawrence, J.R., Swerhone, G.D.W., Korber, D.R., 2012. Spatial variation in microbial community structure, richness, and diversity in an alluvial aquifer. Can. J. Microbiol. 58, 1135–1151. https://doi.org/10.1139/w2012-087.

Müller, R.H., Rohwerder, T., Harms, H., 2008. Degradation of fuel oxygenates and their main intermediates by *Aquincola tertiaricarbonis* L108. Microbiology 154, 1414–1421. https://doi.org/10.1099/mic.0.2007/014159-0.

Pannier, A., Oehm, C., Fischer, A.R., Werner, P., Soltmann, U., Böttcher, H., 2010. Biodegradation of fuel oxygenates by sol-gel immobilized bacteria *Aquincola tertiaricarbonis* L108. Enzyme Microb. Technol. 47, 291–296. https://doi.org/10.1016/j.enzmictec.2010.07.014.

Pickup, R., Rhodes, G., Alamillo, M., Mallinson, H.E., Thornton, S., Lerner, D., 2001. Microbiological analysis of multi-level borehole samples from a contaminated groundwater system. J. Contam. Hydrol. 53, 269–284. https://doi.org/10.1016/S0169-7722(01)00169-3.

Purswani, J., Juárez, B., Rodelas, B., Gónzalez-López, J., Pozo, C., 2011. Biofilm formation and microbial activity in a biofilter system in the presence of MTBE, ETBE and TAME. Chemosphere 85, 616–624. https://doi.org/10.1016/j.chemosphere.2011.06.106.

R Core Team, 2018. R: A Language and Environment for Statistical Computing. R Foundation for Statistical Computing, Vienna, Austria.

Rohwerder, T., Breuer, U., Benndorf, D., Lechner, U., Müller, R.H., 2006. The alkyl *tert*-butyl ether intermediate 2-hydroxyisobutyrate is degraded via a novel cobalamin-dependent mutase pathway. Appl. Environ. Microbiol. 72, 4128–4135. https://doi.org/10.1128/AEM.00080-06.

Rosell, M., Barceló, D., Rohwerder, T., Breuer, U., Gehre, M., Richnow, H.H., 2007. Variations in13C/12C and D/H enrichment factors of aerobic bacterial fuel oxygenate degradation. Environ. Sci. Technol. 41, 2036–2043. https://doi.org/10.1021/es0616175.

Schmidt, R., Battaglia, V., Scow, K., Kane, S., Hristova, K.R., 2008. Involvement of a novel enzyme, MdpA, in methyl *tert*-butyl ether degradation in *Methylibium petroleiphilum* PM1. Appl. Environ. Microbiol. 74, 6631–6638. https://doi.org/10.1128/AEM.01192-08.

Schuster, J., Schäfer, F., Hübler, N., Brandt, A., Rosell, M., Härtig, C., Harms, H., Müller, R.H., Rohwerder, T., 2012. Bacterial degradation of *tert*-amyl alcohol proceeds via hemiterpene 2-methyl-3-buten-2-ol by employing the tertiary alcohol desaturase function of the Rieske nonheme mononuclear iron oxygenase MdpJ. J. Bacteriol. 194, 972–981. https://doi.org/10.1128/JB.06384-11.

Schuster, J., Purswani, J., Breuer, U., Pozo, C., Harms, H., Müller, R.H., Rohwerder, T., 2013. Constitutive expression of the cytochrome P450 EthABCD monooxygenase system enables degradation of synthetic dialkyl ethers in *Aquincola tertiaricarbonis* L108. Appl. Environ. Microbiol. 79, 2321–2327. https://doi.org/10.1128/AEM.03348-12.

Shah, N.W., Thornton, S.F., Bottrell, S.H., Spence, M.J., 2009. Biodegradation potential of MTBE in a fractured chalk aquifer under aerobic conditions in long-term uncontaminated and contaminated aquifer microcosms. J. Contam. Hydrol. 103, 119–133. https://doi.org/10.1016/j.jconhyd.2008.09.022.

Shih, T., Rong, Y., Harmon, T., Suffet, M., 2004. Evaluation of the impact of fuel hydrocarbons and oxygenates on groundwater resources. Environ. Sci. Technol. 38, 42–48. https://doi.org/10.1021/es0304650.

Stafford, B.P., Rixey, W.G., 2012. Distribution of fuel-grade ethanol near a dynamic water table. Ground Water Monit. Remediat. 32, 42–52. https://doi.org/10.1111/j1745.

Stupp, D., Gass, M., Leiteritz, H., Pijls, C., Thornton, S., Smith, J., Dunk, M., Grosjean, T., Den Haan, K., 2012. Gasoline Ether Oxygenate Occurrence in Europe, and a Review of Their Fate and Transport Characteristics in the Environment. CONCAWE Report 4/12s.

Szabó, Z., Gyula, P., Robotka, H., Bató, E., Gálik, B., Pach, P., Pekker, P., Papp, I., Bihari, Z., 2015. Draft genome sequence of *Methylibium* sp. strain T29, a novel fuel oxygenate-degrading bacterial isolate from Hungary. Stand. Genomic Sci. 10, 39. https://doi.org/10.1186/s40793-015-0023-z.

Thornton, S.F., Quigley, S., Spence, M.J., Banwart, S.A., Bottrell, S., Lerner, D.N., 2001. Processes controlling the distribution and natural attenuation of dissolved phenolic compounds in a deep sandstone aquifer. J. Contam. Hydrol. 53, 233–267. https://doi.org/10.1016/S0169-7722(01)00168-1.

Tuxen, N., Albrechtsen, H.-J., Bjerg, P.L., 2006. Identification of a reactive degradation zone at a landfill leachate plume fringe using high resolution sampling and incubation techniques. J. Contam. Hydrol. 85, 179–194. https://doi.org/10.1016/j.jconhyd.2006.01.004.

van der Waals, M.J., Pijls, C., Sinke, A.J.C., Langenhoff, A.A.M., Smidt, H., Gerritse, J., 2018. Anaerobic degradation of a mixture of MtBE, EtBE, TBA, and benzene under different redox conditions. Appl. Microbiol. Biotechnol. 102, 3387–3397. https://doi.org/10.1007/s00253-018-8853-4.

van der Waals, M.J., Plugge, C., Meima-Franke, M., de Waard, P., Bodelier, P.L.E., Smidt, H., Gerritse, J., 2019. Ethyl *tert*-butyl ether (EtBE) degradation by an algal-bacterial culture obtained from contaminated groundwater. Water Res. 148, 314–323. https://doi.org/10.1016/j.watres.2018.10.050.

van Wezel, A., Puijker, L., Vink, C., Versteegh, A., de Voogt, P., 2009. Odour and flavour thresholds of gasoline additives (MTBE, ETBE and TAME) and their occurrence in Dutch drinking water collection areas. Chemosphere 76, 672–676. https://doi.org/10.1016/j.chemosphere.2009.03.073.

Xu, Z., Chai, J., Wu, Y., Qin, R., 2015. Transport and biodegradation modeling of gasoline spills in soil–aquifer system. Environ. Earth Sci. 74, 2871–2882. https://doi.org/10.1007/s12665-015-4311-0.

Yeh, C.K., Novak, J.T., 1994. Anaerobic biodegradation of gasoline oxygenates in soils. Water Environ. Res. 66, 744–752.